1   Identification of a genetic element required for spore killing in Neurospora

2

3   Nicholas A. Rhoades*, Austin M. Harvey*[,1], Dilini A. Samarajeewa*[,1], Jesper Svedberg[†],

4   Aykhan Yusifov*, Anna Abusharekh*, Pennapa Manitchotpisit*, Daren W. Brown[‡], Kevin J.

5   Sharp*, David G. Rehard[§,**], Joshua Peters*, Xavier Ostolaza-Maldonado*, Jackson

6   Stephenson*, Patrick K. T. Shiu[§], Hanna Johannesson[†], and Thomas M. Hammond*[,2]

7

8   *School of Biological Sciences, Illinois State University, Normal, Illinois, 61790

9   [†]Department of Organismal Biology, Uppsala University, Uppsala, Sweden

10   [‡]Mycotoxin Prevention and Applied Microbiology, National Center for Agricultural Utilization

11   Research, U.S. Department of Agriculture, Agricultural Research Service, Peoria, Illinois 61604

12   [§]Division of Biological Sciences, University of Missouri, Columbia, Missouri, 65211

13   [**]Department of Biology, University of Iowa, Iowa City, Iowa 52242

14

15   [1]These authors contributed equally to this work.

16

17   [2]Corresponding author:

18   Thomas M. Hammond

19   346 Science Laboratory Building

20   Illinois State University

21   Normal, IL 61790

22   Phone: 309-438-2602

23   Email: tmhammo@ilstu.edu

24   Running title

25   A spore killing gene in Neurospora

26

27   KEYWORDS

28   meiotic drive, transmission ratio distortion, spore killing, MSUD

29

30   [2]Corresponding author: Illinois State University, School of Biological Sciences, 346 Science

31   Laboratory Building, Normal, IL 61790. E-mail: tmhammo@ilstu.edu.

32

33

34 **ABSTRACT**

35   Meiotic drive elements like *Spore killer-2* (*Sk-2*) in Neurospora are transmitted through sexual

36   reproduction to the next generation in a biased manner. *Sk-2* achieves this biased transmission

37   through spore killing. Here, we identify *rfk-1* as a gene required for the spore killing mechanism.

38   The *rfk-1* gene is associated with a 1,481 bp DNA interval (called *AH36*) near the right border of

39   the 30 cM *Sk-2* element, and its deletion eliminates the ability of *Sk-2* to kill spores. The *rfk-1*

40   gene also appears to be sufficient for spore killing because its insertion into a non-*Sk-2* isolate

41   disrupts sexual reproduction after the initiation of meiosis. Although the complete *rfk-1*

42   transcript has yet to be defined, our data indicate that *rfk-1* encodes a protein of at least 39 amino

43   acids and that *rfk-1* has evolved from a partial duplication of gene *ncu07086*. We also present

44   evidence that *rfk-1*'s location near the right border of *Sk-2* is critical for the success of spore

45   killing. Increasing the distance of *rfk-1* from the right border of *Sk-2* causes it to be inactivated

46   by a genome defense process called meiotic silencing by unpaired DNA (MSUD), adding to

47   accumulating evidence that MSUD exists, at least in part, to protect genomes from meiotic drive.

48

49

INTRODUCTION

50

51   In eukaryotic organisms, genetic loci are typically transmitted through sexual reproduction to the

52   next generation in a Mendelian manner. However, some loci possess the ability to improve their

53   own transmission rate through meiosis at the expense of a competing locus. These "selfish" loci

54   are often referred to as meiotic drive elements (Zimmering *et al.* 1970). The genomic conflict

55   caused by meiotic drive elements may impact processes ranging from gametogenesis to

56   speciation (Lindholm *et al*. 2016). Meiotic drive elements are found across the eukaryote tree of

57   life (Burt and Trivers 2008; Bravo Núñez *et al*. 2018) and classic examples include *SD* in fruit

58   flies (Larracuente and Presgraves 2012), the *t*-complex in mice (Lyon 2003; Sugimoto 2014),

59   and *Ab10* in *Zea mays* (Rhoades 1952; Kanizay *et al.* 2013). In the fungal kingdom, the known

60   meiotic drive elements achieve biased transmission through spore killing (Raju 1994) and a

61   handful of spore killer systems have been studied in detail. While the prion-based spore killing

62   mechanism of *het-s* in *Podospora anserina* is the best characterized (Dalstra *et al.* 2003; Saupe

63   2011), the mechanisms by which other fungal meiotic drive elements kill spores are mostly

64   unknown (*e.g.*, see Grognet et al. 2014; Hu et al. 2017; Nuckolls et al. 2017).

65

66   Two fungal meiotic drive elements have been identified in the fungus *Neurospora*

67   *intermedia* (Turner and Perkins, 1979). This species is closely related to the genetic model

68   *Neurospora crassa* (Davis 2000), and the mating processes in both fungi are essentially identical.

69   Mating begins with fertilization of an immature fruiting body called a protoperithecium by a

70   mating partner of the opposite mating type. After fertilization, the protoperithecium develops

71   into a mature fruiting body called a perithecium. The nuclei from each parent multiply within the

72   developing perithecium, and a single nucleus from each parent is sequestered into a tube-like

73 meiotic cell (Raju 1980). Meiosis begins with fusion of the parental nuclei and ends with

74 production of four recombinant daughter nuclei. Each recombinant nucleus proceeds through a

75 single round of mitosis, resulting in a total of eight nuclei in the meiotic cell. A process known as

76 ascosporogenesis then constructs cell walls and membranes around each nucleus to produce

77 sexual spores called ascospores. Maturing ascospores accumulate a dark pigment and develop

78 the shape of a spindle; thus, at the end of ascosporogenesis, the mature meiotic cells appear to

79 contain eight miniature black American footballs (Figure 1A). The meiotic cells also serve as

80 ascospore sacs (asci) and a single perithecium can produce hundreds of asci, each derived from a

81 unique meiotic event.

82

83   During an effort in the 1970s to collect and characterize *Neurospora* isolates from around

84 the world, Turner and Perkins discovered pairs of compatible mating partners that did not

85 produce asci with eight viable ascospores (Perkins 1974; Turner and Perkins 1979). This

86 outcome was more common when crosses were performed between isolates from widely

87 separated populations, and in some cases the abnormal asci were attributed to heterozygosity of

88 chromosome rearrangements between mating partners. However, for a few isolates of *N.*

89 *intermedia*, asci with atypical phenotypes were due to chromosomal factors called *Spore killer-2*

90 (*Sk-2*) and *Spore killer-3* (*Sk-3*). *Sk-2* and *Sk-3* are not single genes; rather, they are complexes of

91 genes that span approximately 30 cM of chromosome III, and they are transmitted through

92 meiosis as single units due to a recombination suppression mechanism thought to be enforced by

93 inversions (Turner and Perkins 1979; Campbell and Turner 1987; Hammond *et al.* 2012; Harvey

94 *et al.* 2014). Unlike standard genetic elements, which display a Mendelian transmission rate of

95 50% through sexual reproduction, *Sk-2* and *Sk-3* are transmitted at levels approaching 100%

96 (Turner and Perkins 1979). This biased transmission occurs because *Sk-2* and *Sk-3* kill

97 ascospores that do not inherit resistance to spore killing (Raju 1979; Turner and Perkins 1979).

98 For example, in *Sk-2* × *Spore killer*-sensitive (Sk^S) crosses, asci with four black ascospores and

99 four clear ("white") ascospores are produced (Figure 1A). This phenotype can be symbolized as

100 4B:4W. The four black ascospores are typically viable and nearly always of the *Sk-2* genotype,

101 while the four white ascospores are inviable and presumed to be of the Sk^S genotype. The same

102 phenomenon occurs in *Sk-3* × Sk^S crosses, except the four black ascospores are of the *Sk-3*

103 genotype.

104

105   Although spore killers have not yet been detected in wild isolates of *N. crassa*, *Sk-2* and

106 *Sk-3* have been introgressed into this species for genetic analysis. Introgression of *Sk-2* and *Sk-3*

107 has allowed the discovery of resistance to spore killing in natural populations of *N. crassa*

108 (Turner and Perkins 1979; Turner 2001). One of the *Sk-2*-resistant isolates (FGSC 2222) carries

109 a resistant version of a gene whose function is best described by its name: *resistant to Spore*

110 *killer* (*rsk*). Crosses of rsk^{LA} × *Sk-2*, where rsk^{LA} is the Louisiana allele of *rsk* carried by FGSC

111 2222, produce asci with an 8B:0W phenotype because ascospores inherit either rsk^{LA} or *Sk-2,* and

112 both are sufficient for resistance to *Sk-2*-based spore killing (Hammond *et al.* 2012). Discovery

113 of rsk^{LA} made identifying other *rsk* alleles possible, some of which do not provide resistance to

114 the known spore killers. For example, the Oak Ridge *rsk* allele (rsk^{OR}), typical of most laboratory

115 strains, is resistant to neither *Sk-2* nor *Sk-3*. Additionally, some *rsk* alleles confer resistance to

116 *Sk-3* but not *Sk-2*. An example is rsk^{PF5123}, which exists in an *N. intermedia* isolate from French

117 Polynesia. *Sk-2* and *Sk-3* also carry resistant versions of *rsk*, referred to as rsk^{Sk-2} and rsk^{Sk-3},

118 respectively. Crosses homozygous for *Sk-2* (*i.e., Sk-2* × *Sk-2*) or *Sk-3* produce asci with an

119   8B:0W phenotype because each ascospore inherits a resistant *rsk* allele. Furthermore,

120   heterozygous crosses between different spore killers (*e.g.*, *Sk-2* × *Sk-3*) produce asci with a

121   0B:8W phenotype (Turner and Perkins 1979) because each ascospore inherits either rsk^{Sk-2} or

122   rsk^{Sk-3} but not both (and rsk^{Sk-2} ascospores are killed by *Sk-3* while rsk^{Sk-3} ascospores are killed by

123   *Sk-2*).

124

125   The Killer-Neutralization (KN) model has been proposed to explain how *Sk-2* and *Sk-3*

126   achieve biased transmission through sexual reproduction (Hammond *et al.* 2012). The KN model

127   holds that *Sk-2* and *Sk-3* each use a resistance protein and a killer protein (or nucleic acid) and

128   both proteins are active throughout meiosis and ascosporogenesis. During the early stages of

129   meiosis, in an Sk^S × *Sk-2* (or *Sk-3*) cross, both the resistance protein and the killer protein are

130   hypothesized to diffuse throughout the meiotic cell. This unrestricted movement allows the

131   resistance protein to neutralize the killer protein wherever the latter protein may be found.

132   However, once ascospores are separated from the cytoplasm, the resistance protein becomes

133   restricted to those ascospores that produce it (*e.g.*, *Sk-2* ascospores), and ascospores that do not

134   carry a resistant version of *rsk* (*e.g.*, Sk^S ascospores) are subsequently killed. This model requires

135   the killer protein to move between ascospores after ascospore delimitation or to have a long

136   half-life that allows it to remain functional in sensitive ascospores.

137

138   Evidence for the KN model is seen in the outcome of Sk^S × *Sk-2* $rsk^{\Delta Sk-2}$ crosses, where

139   the latter strain has been deleted of its *rsk* allele. These crosses do not produce ascospores;

140   instead, they produce asci that abort meiosis before ascospore production (Hammond *et al.*

141   2012). Meiotic cells of these crosses lack a resistant RSK, which likely causes the killing process

7

142   to begin early in meiosis (at the ascus level) rather than during ascosporogenesis (at the

143   ascospore level). The KN model is also supported by the existence of different *rsk* alleles.

144   Previous studies have demonstrated the sequence of RSK to be the most important factor towards

145   determining which killer it neutralizes (Hammond *et al.* 2012), suggesting that RSK and the

146   killer may interact by a "lock and key" mechanism. To test this hypothesis, the killer must first

147   be identified.

148

149   As described above, $Sk^S \times Sk\text{-}2\ rsk^{\Delta Sk\text{-}2}$ crosses produce abortive asci. We recently used

150   this characteristic to screen for mutations that disrupt spore killing (Harvey *et al.* 2014).

151   Specifically, we fertilized an Sk^S mating partner with mutagenized $Sk\text{-}2\ rsk^{\Delta Sk\text{-}2}$ conidia (asexual

152   spores that also function as fertilizing propagules). We reasoned that only an $Sk\text{-}2\ rsk^{\Delta Sk\text{-}2}$

153   conidium mutated in a gene "*r*equired *f*or spore *k*illing" (*rfk*) would produce viable ascospores

154   when crossed with Sk^S. The screen allowed us to isolate six *rfk* mutants (ISU-3211 through

155   ISU-3216). Complementation analysis of each mutant strain suggested all to be mutated at the

156   same locus, which was subsequently named *rfk-1* and mapped to a 45 kb region within *Sk-2* on

157   chromosome III. Here, we report the identification of *rfk-1* as a gene encoding a protein of at

158   least 39 amino acids. In addition to identifying *rfk-1*, we have found that the cellular process of

159   meiotic silencing by unpaired DNA places limits on the location of *rfk-1* within *Sk-2*. The

160   implications of this finding with respect to meiotic drive element evolution are discussed.

161

162 **MATERIALS AND METHODS**

163 **Strains, media, and crossing conditions**

164 The strains used in this study are listed along with genotype information in Table 1. Vogel's

165 minimum medium (Vogel 1956), with supplements as required, was used to grow and maintain

166 all strains. Hygromycin B and nourseothricin sulfate (Gold Biotechnology) were used at a

167 working concentration of 200 μg / ml and 45 μg / ml, respectively. Synthetic crossing medium

168 (pH 6.5) with 1.5% sucrose, as described by Westergaard and Mitchell (1947), was used for

169 crosses. Crosses were unidirectional and performed on a laboratory benchtop at room

170 temperature under ambient lighting (Samarajeewa *et al.* 2014). After fertilization, crosses were

171 allowed to mature for 12-16 days before perithecial dissection in 25 or 50% glycerol and asci

172 were examined with a standard compound light microscope and imaging system. Ascus

173 phenotype designations were based on qualitative observations. More than 90% of the asci from

174 a cross had to display the same phenotype to receive one of the following designations: 8B:0W,

175 4B:4W, or aborted.

176

177 **Genetic modification of *N. crassa*, genotyping, and sequence confirmations**

178 A technique called double-joint PCR was used to construct all deletion vectors (Yu *et al.* 2004;

179 Hammond *et al.* 2011). Transgene-insertion vectors were designed to insert transgenes along

180 with a hygromycin resistance cassette (*hph*) next to *his-3* on chromosome I. Construction details

181 for deletion and insertion vectors are provided in Supporting Information (Tables S1–S4).

182 Transformations of *N. crassa* were performed by electroporation of conidia (Margolin *et al*.

183 1997). Homokaryons were derived from heterokaryotic transformants with a microconidium

184 isolation technique (Ebbole and Sachs, 1990) or by crossing the transformants to standard

9

185   laboratory strains (F2-23 or F2-26) to obtain homokaryotic ascospores. Site-directed mutagenesis

186   was performed essentially as described for the QuikChange II Site-Directed Mutagenesis Kit

187   (Revision E.01, Agilent Technologies) and details for its use are provided in Table S5. All

188   genotypes were confirmed by polymerase chain reaction (PCR) assays on genomic DNA isolated

189   from lyophilized (freeze-dried) mycelia with IBI Scientific's Mini Genomic DNA Kit

190   (Plant/Fungi). Sanger sequencing was used to confirm sequences and/or identify mutations in

191   PCR products and plasmids.

192

193   **Data availability**

194   All strains and plasmids generated during this study are available upon request. Supplemental

195   files available at FigShare.

10

196   **RESULTS**

197   **Deletion of a DNA interval spanning most of $Sk\text{-}2^{INS1}$ eliminates spore killing**

198   The annotated 45 kb *rfk-1* region contains 14 protein-coding genes, two pseudogenes (denoted

199   with an asterisk), an inverted sequence ($Sk\text{-}2^{INV1}$), an inversion breakpoint, and an 11 kb

200   insertion sequence ($Sk\text{-}2^{INS1}$; GenBank: KJ908288.1; Figure 1B). To refine the location of *rfk-1*

201   within this 45 kb region, intervals *v3*, *v4*, and *v5* (Figure 1B and Table 2) were deleted and

202   replaced with *hph* and the resulting deletion strains were crossed with an Sk^S mating partner. We

203   found that while deletion of interval *v3* or *v4* had no effect on spore killing (asci are 4B:4W;

204   Figure 1, C and D), deletion of *v5* eliminated it (asci are 8B:0W; Figure 1E).

205

206   **A DNA interval between $ncu07838^*$ and $ncu06238$ is required for spore killing**

207   Interval *v5* spans most of $Sk\text{-}2^{INS1}$ (Figure 2, A and B). To further refine the position of *rfk-1*

208   within $Sk\text{-}2^{INS1}$, we constructed nine additional deletion strains and crossed each one with an Sk^S

209   mating partner (Figure 2B and Table 2). Surprisingly, deletion of the annotated genes and

210   pseudogenes within $Sk\text{-}2^{INS1}$ did not interfere with spore killing (Figure 3, A–D). In contrast,

211   deletion of the intergenic region between *ncu07838** and *ncu06238* eliminated spore killing

212   (Figure 3, E–I).

213

214   **An ascus aborting element exists between $ncu07838^*$ and $ncu06238$**

215   The above results suggest that *rfk-1* is found within the intergenic region between $ncu07838^*$ and

216   *ncu06238* and that *rfk-1* is required for spore killing. But, is *rfk-1* also sufficient for spore

217   killing? To answer this question, we genetically-modified eight Sk^S strains to carry different

218   intervals of $Sk\text{-}2^{INS1}$ (Figure 2C and Table 2) and found that each strain produced normal asci

11

219   when crossed with an Sk^S mating partner (Figure S1). The reason for this finding can be traced to

220   a silencing process called meiotic silencing by unpaired DNA (MSUD; Hammond 2017;

221   Aramayo and Selker 2013). In a standard cross, where only one mating partner carries an ectopic

222   transgene (*e.g.*, an interval of Sk-2^{INS1}), MSUD identifies the transgene as unpaired and silences

223   it for the duration of meiosis. Therefore, to detect a phenotype that requires the expression of an

224   unpaired transgene during meiosis, it is often necessary to suppress MSUD. MSUD suppression

225   can be achieved by deleting a gene called *sad-2* from one mating partner of a cross (Shiu *et al.*

226   2006). With this technique, we found that some Sk-2^{INS1} intervals have no effect on ascus

227   development, while others abort it. For example, normal asci are produced by strains carrying

228   intervals $AH4^{Sk-2}$, $AH6^{Sk-2}$, $AH14^{Sk-2}$, or $AH32^{Sk-2}$ (Figure 4, A–C and H), while aborted asci are

229   produced by strains carrying intervals $AH30^{Sk-2}$, $AH31^{Sk-2}$, $AH36^{Sk-2}$, or $AH37^{Sk-2}$ (Figure 4, D–G).

230   The ascus abortion phenotype can be explained by the presence of *rfk-1* without the presence of a

231   resistant version of *rsk*. Taken together, these findings suggest that intervals $AH30^{Sk-2}$, $AH31^{Sk-2}$,

232    $AH36^{Sk-2}$, and $AH37^{Sk-2}$ contain *rfk-1* and that *rfk-1* is sufficient for spore killing.

233

234   **The *AH36* interval from an *rfk-1* strain does not cause ascus abortion**

235   The shortest abortion-inducing interval identified by the above experiments is *AH36*, located

236   between positions 27,899 and 29,381 of the 45 kb *rfk-1* region (Figure 2C and Table 2). Because

237   the research path that led us to *AH36* began with mapping the position of *rfk-1* in strain

238   ISU-3211 (Harvey *et al.* 2014), *AH36* in ISU-3211 (referred to as $AH36^{3211}$) should harbor at

239   least one mutation that disrupts *rfk-1* function. To test this hypothesis, we transferred $AH36^{3211}$ to

240   an Sk^S genetic background and crossed the resulting strain with an Sk^S sad-2^Δ mating partner. As

241   expected, we found that Sk^S sad-$2^\Delta \times Sk^S$ $AH36^{3211}$ crosses produce normal asci (Figure 5).

242

The G28326A mutation disrupts the ascus-aborting ability of *AH36^{Sk-2}*

The different phenotypes associated with *AH36^{Sk-2}* and *AH36^{3211}* suggest that they differ at the

sequence level. Indeed, sequencing of these two alleles allowed us to identify seven guanine to

adenine transition mutations in *AH36^{3211}* (Figure 6A; G27904A, G27945A, G27972A, G28052A,

G28104A, G28300A, and G28326A). To determine if one (or more) of these mutations is

responsible for the inability of *AH36^{3211}* to cause ascus abortion, we examined six of the seven

mutations by site-directed mutagenesis. For each mutation, this involved mutating the base in a

clone of interval *AH36^{Sk-2}*, placing the mutated interval (*e.g.*, *AH36^{Sk-2[G27945A]}*) in an *Sk^S* strain, and

crossing the transgenic strain to an *Sk^S sad-2^Δ* mating partner. Through this procedure, we found

that only one of the six mutations examined (*i.e.,* G28326A) eliminates the ascus-aborting ability

of *AH36^{Sk-2}* (Figure 7).

254

We also identified a 46–48 bp tandem repeat (7.17 repeats) between positions 28,384 and

28,722 (Figure 6, A and B). The sequences of *AH36^{Sk-2}* and *AH36^{3211}* are identical between these

positions and thus the biological significance of the tandem repeats with respect to spore killing

is currently unknown.

259

A putative start codon for RFK-1 is located within *AH36*

The G28326A mutation is 62 bp to the right of a putative start codon at position 28,264 (Figure

6). To test if this "ATG" could serve as the start codon for RFK-1, we constructed two deletion

vectors: v199 and v200 (Figure 8A). Vector v199 deletes the interval between 28,131 and 28,264

and replaces it with *hph* and the promoter of the *N. crassa ccg-1* gene, thereby inserting

13

265   *hph-ccg-1*(P) directly upstream of the ATG at position 28,264 (Figure 8B). As a control, we used

266   vector v200 to place *hph-ccg-1*(P) directly upstream of position 28,354, located 90 bases to the

267   right of the proposed *rfk-1* start codon. When inserted directly upstream of 28,264, *hph-ccg-1*(P)

268   has no effect on spore killing (Figure 8, C and D). In contrast, when inserted 90 bases to the right

269   of this position, *hph-ccg-1*(P) disrupts spore killing (Figure 8E). These findings demonstrate that

270   the ATG at position 28,264 could serve as the *rfk-1* start codon. Furthermore, they suggest that

271   placement of *hph-ccg-1*(P) directly upstream of position 28,354 interrupts the *rfk-1* coding

272   region.

273

274   **The arrangement of *rfk-1* within *Sk-2* protects it from MSUD**

275   The right border of *Sk-2* is found at position 29,151 (Figure 9A, dotted line; Table 2; Harvey *et*

276   *al.* 2014). To the right of this position, the sequences of *Sk-2* and *Sk^S* strains are very similar. For

277   example, a simple ClustalW alignment (Thompson *et al.* 1994; Hall 1999) finds that *Sk-2*

278   positions 29,152 through 35,728 are 94.4% identical to the corresponding positions within *Sk^S*

279   (GenBank: CM002238.1, positions 2,011,073 to 2,017,662). In contrast, the sequences to the left

280   of the *Sk-2* border are unrelated between *Sk-2* and *Sk^S* strains (Figure 9A). Interestingly, most of

281   *AH36* is found to the left of the *Sk-2* border, and thus most of *AH36*, including *rfk-1*, is unpaired

282   during meiosis in *Sk^S* × *Sk-2* crosses. If so, how does *rfk-1* avoid inactivation by MSUD? While

283   the molecular details of how MSUD detects unpaired DNA are unknown, we considered the

284   possibility that the distance of *rfk-1* from a "paired" sequence allows it to avoid MSUD (*e.g.*, see

285   the *ncu06238* genes in *Sk-2* and *Sk^S*, Figure 9A). To test this hypothesis, we inserted *hph*

286   immediately to the right of *AH36* in a standard *Sk-2* strain (Figure 9A). We refer to this particular

287   allele as *v140$^\Delta$::hph*. The *v140$^\Delta$::hph* allele increases the distance of *rfk-1* from paired sequences

14

288   by a length of 1391 bp (the length of *hph* minus the 21 bp that were deleted by v140). As

289   predicted, we found that spore killing is absent in $Sk^S \times Sk$-2 $v140^\Delta$::*hph* crosses (Figure 9B). To

290   confirm that the lack of spore killing is a result of the increased distance of *rfk-1* from paired

291   DNA during meiosis, we inserted *hph* at the corresponding location in an Sk^S strain (Figure 9A).

292   We refer to this allele as $v150^\Delta$::*hph*. When an Sk^S $v150^\Delta$::*hph* strain is crossed with an *Sk-2*

293     $v140^\Delta$::*hph* strain, spore killing is normal (Figure 9C). Thus, the proximity of *rfk-1* to paired

294   DNA helps it avoid inactivation by MSUD. As a final test of this hypothesis, we crossed Sk^S

295   sad-2^Δ and *Sk-2* $v140^\Delta$::*hph* mating partners and found that spore killing is also normal in this

296   cross (Figure 9D), most likely because sad-2^Δ suppresses MSUD, which makes the distance of

297   *rfk-1* from paired sequences irrelevant to the expression of *rfk-1* during meiosis.

298

299   **The *rfk-1* gene does not include *ncu06238***

300   To confirm that *ncu06238*, the gene to the right of *rfk-1* (as depicted in Figure 10A), is not

301   required for spore killing, we deleted *ncu06238* from both Sk^S and *Sk-2* and analyzed ascus

302   phenotypes in crosses involving *ncu06238* deletion strains. However, we found that Sk^S

303     $ncu06238^\Delta \times Sk^S$ crosses produce asci with varying numbers of fully developed ascospores

304   (Figure 10A). Therefore, we could not use ascus phenotype to determine if spore killing is

305   functional in Sk^S $ncu06238^\Delta \times Sk$-2 $ncu06238^\Delta$ crosses (Figure 10B). Instead, we calculated the

306   percentage of progeny with an *Sk-2* genotype produced by a cross between Sk^S $ncu06238^\Delta$ and

307   *Sk-2* $ncu06238^\Delta$ mating partners. We found that 46 of 47 progeny had the *Sk-2* genotype (data

308   not shown). Therefore, because meiotic drive functions without *ncu06238*, the *rfk-1* coding

309   region does not overlap or include positions occupied by *ncu06238*.

310

15

311 **Replacement of *AH36*[3211] with *AH36*[Sk-2] restores spore killing to an *rfk-1* mutant**

312 The *rfk-1* mutant strain ISU-3211 carries seven mutations within its *AH36* interval (Figure 6). To

313 confirm that at least one of these mutations (presumably G28326A) is responsible for

314 ISU-3211's inability to kill ascospores, we replaced *AH36*[3211] in a descendant of ISU-3211

315 (strain ISU-3222) with *AH36*[Sk-2]*::hph* (Figure 11A and Table S4). Because the presence of an

316 *hph* marker to the right of *AH36* disrupts spore killing in an MSUD-dependent manner (Figure

317 9B), we performed our test crosses with both a standard Sk^S mating partner and an Sk^S

318 $v150^A::hph$ mating partner. As expected, we found that replacing *AH36*[3211] with *AH36*[Sk-2]

319 restores spore killing to a spore killing-deficient strain (Figure 11, B–G). These results

320 demonstrate that the *AH36*[3211] interval is responsible for the loss of spore killing in ISU-3211 and

321 its *rfk-1* descendants.

322

323 **The RFK-1 protein contains (at least) 39 amino acids**

324 Assuming that the start codon for RFK-1 begins at position 28,264, and that the pre-mRNA for

325 *rfk-1* includes no introns (see discussion), we can propose the following hypothesis: RFK-1 is a

326 39 amino acid protein encoded by DNA located between positions 28,263 and 28,384 (Table 2

327 and Figure 12A). We found support for this hypothesis by sequencing the *AH36* intervals in

328 strains ISU-3211 through ISU-3216 (Figure 12A), which are the six *Sk-2 rfk-1* isolates obtained

329 by our initial screen for spore killing-deficient mutants (Harvey *et al.* 2014). Specifically, we

330 found that *AH36*[3211] contains the previously discussed G28326A mutation, which changes the

331 21st codon from a tryptophan codon to a stop codon; *AH36*[3212] contains an extra thymine within a

332 run of six thymines between positions 28,281 and 28,288, which causes a frameshift mutation in

333 the 9th *rfk-1* codon; and *AH36*[3213] contains a G28348A mutation, which changes the 29th codon

16

334   from an alanine codon to a threonine codon. In addition, we found that the sequences of

335   *AH36*^{3214}, *AH36*^{3215}, and *AH36*^{3216}, are all identical to the sequence of *AH36*^{3211}, suggesting that

336   ISU-3211, ISU-3214, ISU-3215, and ISU-3216 were all "fathered" by the same mutagenized

337   conidium. In all, we identified at least one potential codon-altering mutation between positions

338   28,263 and 28,384 in each of the six known *rfk-1* mutants. This strongly suggests that the

339   interval between positions 28,263 and 28,384 contains at least part, if not all, of the RFK-1

340   coding sequence.

341

342   **RFK-1 is related to NCU07086**

343   To investigate the origin of *rfk-1*, we downloaded a list of predicted *N. crassa* proteins from the

344   National Center for Biotechnology Information (NCBI)'s Genome Database (Accession No.

345   GCA_000182925.2) and performed a BLASTP search (Camacho *et al.* 2009) on the list with the

346   hypothetical 39 aa RFK-1 sequence as query (Figure 12A). We found that the most significant

347   match (Expect = 2e-7) to RFK-1 is a hypothetical 362-aa protein called NCU07086 (NCBI

348   Protein Database: XP_960351.1). NCU07086 is encoded by the *ncu07086* gene on *N. crassa*

349   chromosome VI and is predicted to contain four introns (Figure 12B, I1 through I4; NCBI Gene

350   Database, 3876500). A search of NCBI's conserved domain database (CDD v3.16;

351   Marchler-Bauer *et al.* 2015) with the predicted sequence of NCU07086 identified a region with a

352   low-scoring match to the AtpF Superfamily (Expect=2.32e-3; Figure 12B). Interestingly, RFK-1

353   is highly similar to the first 39 amino acids of NCU07086 (Figure 12C), and it appears that the

354   46–48 bp repeat within *AH36* (Figure 6) expanded from a single 47 bp sequence within

355   *ncu07086*'s first intron (Figure 12D). These findings suggest that *rfk-1* evolved from a partial

356   duplication of the *ncu07086* gene.

17

357   **DISCUSSION**

358   The biological mechanism used by the Neurospora Spore killers to achieve biased transmission

359   is believed to require the action of a resistance protein and a killer protein. In a previous work,

360   we isolated six *rfk* mutants (ISU-3211 through ISU-3216) and provided evidence that each is

361   mutated at the same locus, subsequently named *rfk-1* (Harvey *et al.* 2014). The *rfk-1* locus in

362   ISU-3211 was mapped to a 45 kb region of *Sk-2*. We began this study with the goal of

363   identifying *rfk-1*. At first, we intended to use three point crossing assays to further refine the

364   position of *rfk-1* within the 45 kb *rfk-1* region. These assays were to be performed with *hph*

365   markers inserted between genes *ncu06192* and *ncu06191* (with vector *v3*) and between genes

366   *ncu06239* and *ncu06240* (with vector *v4*); therefore, deletion vectors *v3* and *v4* were designed to

367   delete relatively small intervals from the *rfk-1* region (25 bp and 261 bp, respectively; Table 2)

368   and they were not expected to influence spore killing. Accordingly, they had no effect on spore

369   killing (Figure 1, C and D). In contrast, *v5* was designed to delete a 10,718 bp interval, spanning

370   most of the *Sk-2*$^{\text{INS1}}$ sequence, in hopes that *rfk-1* would be found somewhere within it (Table 2).

371   Fortunately, deletion of interval *v5* (intervals are named after the deletion vectors designed to

372   delete them) was successful and its removal from *Sk-2* eliminated *Sk-2*'s ability to kill ascospores

373   (Figure 1E). We were thus able to focus our efforts on deleting subintervals of *v5,* which allowed

374   us to track *rfk-1* to the intergenic region between *ncu07238** and *ncu06238* (Figures 2, 3, and

375   10)*.*

376

377   We also tested various subintervals of *v5* for the presence of *rfk-1* by transferring them to

378   an *Sk*^{S} strain and performing test crosses with an *Sk*^{S} *sad-2*$^\Delta$ mating partner (Figure 4). For this

379   assay to yield positive results, *rfk-1* must be sufficient for spore killing. Indeed, we found this to

18

380   be the case when we identified four intervals (*AH30*, *AH31, AH37*, and *AH36*) that trigger ascus

381   abortion. These four intervals all have the 1481 bp of *AH36* in common, and the ascus abortion

382   phenotype associated with each interval is likely due to the presence of *rfk-1* without a

383   compatible resistance gene. For example, the KN model holds that the resistance protein (RSK)

384   and the killer are both active during early stages of meiosis (Hammond *et al.* 2012). Lack of a

385   resistant version of RSK, along with expression of the killer, may cause asci to abort meiosis

386   before ascospore delimitation. This phenomenon explains the abortion phenotypes of *AH30*,

387   *AH31,* and *AH37*. However, for succinctness, we also referred to the phenotype associated with

388   *AH36* as ascus abortion, although it may be more accurate to refer to it as a "bubble" phenotype.

389   The bubble phenotype was originally described by Raju *et al*. (1987), and it is thought to arise

390   when asci and/or ascospores abort shortly after ascospore delimitation. Therefore, one

391   explanation for the existence of the two phenotypic classes is that ascus development progresses

392   a bit further with *AH36* than it does with *AH30*, *AH31,* and *AH37*. Asci could progress further

393   with *AH36* if *rfk-1* expression is lower from *AH36* than it is from *AH30*, *AH31,* and *AH37*. In

394   line with this reasoning, *AH36* is the shortest of the abortion-inducing intervals, and, as a result,

395   it may lack some of the regulatory sequences needed for full expression of *rfk-1*. It should be

396   possible to address this hypothesis once the complete transcriptional unit of *rfk-1* is identified.

397

398   Although we have yet to identify *rfk-1*'s transcriptional start (+1) site and termination

399   site, or confirm the presence/absence of introns, we have provided strong evidence that the *rfk-1*

400   coding region includes the DNA interval between positions 28,263 and 28,384 (Figure 6). For

401   example, a putative nonsense mutation at position 28,326 disrupts the ascus-aborting ability of

402   interval *AH36* (Figure 7); spore killing functions when a non-native promoter is attached to the

19

403 putative RFK-1 start codon at position 28,264 (Figure 8); all six of the known *rfk-1* mutants

404 carry putative codon-altering mutations between positions 28,263 and 28,384 (Figure 12A), and

405 insertion of a non-native promoter in the middle of this region disrupts spore killing (Figure 8).

406 However, while our data indicate that the positions between 28,263 and 28,384 are part of the

407 *rfk-1* coding region, they do not eliminate the possibility that the coding sequences for RFK-1

408 include additional positions upstream and/or downstream of 28,263 and 28,384, respectively.

409 Indeed, our preliminary analysis of RNAseq data from $Sk^S \times Sk$-2 crosses (unpublished data)

410 strongly suggests that an intron may exist between positions 28,379 and 28,775. The 5' splice site

411 of this hypothetical intron is related to the 5' splice site of the first intron of *ncu07086* (Figure

412 12D). If this intron does exist within the *rfk-1* pre-mRNA, the RFK-1 stop codon would shift

413 downstream and the length of RFK-1 would increase to 101 aa (assuming position 28,264 is the

414 start codon and no other introns influence the stop codon position). Future work will seek to fully

415 characterize the *rfk-1* coding region by identifying the transcriptional start site, termination site,

416 and any introns that may exist for the primary *rfk-1* transcript, as well as for any biologically

417 significant variants, if they were to exist.

418

419   While this work represents a significant step towards understanding the mechanism of

420 *Sk-2*-based spore killing, many questions remain unanswered. For example, although it appears

421 that RFK-1 evolved from NCU07086, does RFK-1 interfere with NCU07086 function as part of

422 the spore killing mechanism? NCU07086 contains a region with slight homology to the AtpF

423 Superfamily (Figure 12D). Interestingly, the *atpF* gene in *E. coli* (also known as *uncF*; NCBI

424 Gene ID 948247) encodes subunit b of the F-type ATP synthase complex (Walker *et al.* 1984;

425 Dunn 1992; McLachlin and Dunn 1997; Revington *et al.* 1999). This hints that RFK-1 could

20

426   mediate spore killing by targeting eukaryotic F-type ATP synthases, which are associated with

427   mitochondrial membranes in eukaryotes (Stewart *et al.* 2014). However, NCU07086 in *N. crassa*

428   has not been investigated and a much more likely candidate for the b subunit of *N. crassa*'s F-

429   type ATP synthase is found in NCU00502 (KEGG oxidative phosphorylation pathway:

430   ncr00190, release 87.0, Kanehisa and Goto 2000; Kanehisa *et al.* 2016). Thus, at this point in

431   time, a role for RFK-1 in disrupting mitochondrial function as part of the spore killing process is

432   purely speculative.

433

434   Although the primary goal of this work was to identify *rfk-1*, the identity of which has

435   been of interest to meiotic drive researchers since the discovery of *Sk-2* nearly four decades ago,

436   we unexpectedly discovered the strongest evidence to date that genomes in some, if not all,

437   lineages of eukaryotic organisms possess elaborate defense processes to protect themselves from

438   meiotic drive. With respect to Neurospora genomes, this defense process appears to be MSUD.

439   The first hint that MSUD defends Neurospora genomes from meiotic drive appeared in 2007,

440   when it was discovered that *Sk-2* and *Sk-3* are weak MSUD suppressors (Raju *et al.* 2007). Next,

441   in 2012, it was found that the position of *rsk* within *Sk-2* allows it to pair with *rsk* in the Sk^S

442   genome during $Sk\text{-}2 \times Sk^S$ crosses. If *rsk* is not paired during these crosses (*e.g.*, if it is deleted

443   from the Sk^S mating partner), it is silenced by MSUD and the entire ascus is killed by the killer

444   protein, which we now know to be RFK-1. In the current work, we found that the position of

445   *rfk-1* within *Sk-2* is also critical for the success of meiotic drive because it allows *rfk-1* to escape

446   inactivation by MSUD. However, unlike *rsk*, *rfk-1* is only found in *Sk-2* strains and it cannot be

447   paired in $Sk\text{-}2 \times Sk^S$ crosses. Evolution appears to have found a way to circumvent this problem

448   by positioning *rfk-1* close to sequences that are paired during meiosis (*i.e.* close to *ncu06238* in

449   Figure 10). Our data indicate that the proximity of *rfk-1* to paired sequences allows it to escape

450   inactivation by MSUD, which is critical for the success of spore killing. Overall, our findings

451   add to accumulating evidence that MSUD antagonizes the evolution of meiotic drive elements by

452   placing significant constraints on the arrangement of critical genes within the elements.

453   Furthermore, our findings suggest that eukaryotic genomes like those of Neurospora fungi have

454   evolved elaborate defense mechanisms to protect themselves from meiotic drive.

455

456

23

LITERATURE CITED

Aramayo, R., and E. U. Selker, 2013   *Neurospora crassa*, a model system for epigenetics

research. Cold Spring Harb. Perspect. Biol. 5: a017921.

Bravo Núñez, M. A., N. L. Nuckolls, and S. E. Zanders, 2018   Genetic villains: killer meiotic

drivers. Trends Genet. 34: 424–433.

Burt, A., and R. Trivers, 2008   *Genes in Conflict: The Biology of Selfish Genetic Elements*.

Belknap Press of Harvard University Press.

Campbell, J. L., and B. C. Turner, 1987   Recombination block in the Spore killer region of

Neurospora. Genome Natl. Res. Counc. Can. 29: 129–135.

Camacho, C., G. Coulouris, V. Avagyan, N. Ma, J. Papadopoulos *et al.*, 2009   BLAST+:

architecture and applications. BMC Bioinformatics 10: 421.

Dalstra, H. J. P., K. Swart, A. J. M. Debets, S. J. Saupe, and R. F. Hoekstra, 2003   Sexual

transmission of the [Het-S] prion leads to meiotic drive in *Podospora anserina*. Proc.

Natl. Acad. Sci. U. S. A. 100: 6616–6621.

Davis, R. H., 2000   *Neurospora: Contributions of a Model Organism*. Oxford University Press,

USA.

Dunn S. D., 1992   The polar domain of the b subunit of *Escherichia coli* F_1F_0-ATPase forms an

elongated dimer that interacts with the F_1 sector. J. Biol. Chem. 267: 7630–7636.

Ebbole, D., and M. Sachs, 1990   A rapid and simple method for isolation of *Neurospora crassa*

homokaryons using microconidia. Fungal Genet. Newsl. 37: 17–18.

Grognet, P., H. Lalucque, F. Malagnac, and P. Silar, 2014   Genes that bias mendelian

segregation. PLoS Genet 10: e1004387.

494   Hall, T. A., 1999   BioEdit: a user-friendly biological sequence alignment editor and analysis

495   program for Windows 95/98/NT. Nucleic Acid Symp Ser 41: 95–98.

496   Hammond, T. M., 2017 Sixteen years of meiotic silencing by unpaired DNA. Adv. Genet. 97:1–

497   42.

498   Hammond, T. M., D. G. Rehard, H. Xiao, and P. K. T. Shiu, 2012   Molecular dissection of

499   Neurospora Spore killer meiotic drive elements. Proc. Natl. Acad. Sci. U. S. A. 109:

500   12093–12098.

501   Hammond, T. M., H. Xiao, D. G. Rehard, E. C. Boone, T. D. Perdue *et al.*, 2011   Fluorescent

502   and bimolecular-fluorescent protein tagging of genes at their native loci in *Neurospora*

503   *crassa* using specialized double-joint PCR plasmids. Fungal Genet. Biol. 48: 866–873.

504   Harvey, A. M., D. G. Rehard, K. M. Groskreutz, D. R. Kuntz, K. J. Sharp *et al.*, 2014   A critical

505   component of meiotic drive in Neurospora is located near a chromosome rearrangement.

506   Genetics 197: 1165–1174.

507   Hu, W., Z. D. Jiang, F. Suo, J. X. Zheng, W. Z. He, and L. L. Du, 2017   A large gene family in

508   fission yeast encodes spore killers that subvert Mendel's law. ELife Sciences 6, e26057.

509   Kanizay, L. B., T. Pyhäjärvi, E. G. Lowry, M. B. Hufford, D. G. Peterson et al., 2013   Diversity

510   and abundance of the abnormal chromosome 10 meiotic drive complex in *Zea mays*.

511   Heredity 110: 570–577.

512   Kanehisa M., Goto S., 2000   KEGG: kyoto encyclopedia of genes and genomes. Nucleic Acids

513   Res. 28: 27–30.

514   Kanehisa M., Sato Y., Kawashima M., Furumichi M., Tanabe M., 2016   KEGG as a reference

515   resource for gene and protein annotation. Nucleic Acids Res. 44: D457–462.

516 Larracuente, A. M., and D. C. Presgraves, 2012 The selfish *Segregation Distorter* gene

517   complex of *Drosophila melanogaster*. Genetics 192: 33–53.

518 Lindholm, A. K., K. A. Dyer, R. C. Firman, L. Fishman, W. Forstmeier *et al*., 2016 The ecology

519   and evolutionary dynamics of meiotic drive. Trends Ecol. Evol. 31: 315–326.

520 Lyon, M. F., 2003 Transmission ratio distortion in mice. Annu. Rev. Genet. 37: 393–408.

521 Marchler-Bauer, A., M. K. Derbyshire, N. R. Gonzales, S. Lu, F. Chitsaz *et al.*, 2015 CDD:

522   NCBI's conserved domain database. Nucleic Acids Res. 43: D222–226.

523 Margolin, B. S., M. Freitag, and E. U. Selker, 1997 Improved plasmids for gene targeting at the

524   *his-3* locus of *Neurospora crassa* by electroporation. Fungal Genet. Newsl. 44: 34–36.

525 McCluskey, K., A. Wiest, and M. Plamann, 2010 The Fungal Genetics Stock Center: a

526   repository for 50 years of fungal genetics research. J. Biosci. 35: 119–126.

527 McLachlin D. T., Dunn S. D., 1997 Dimerization interactions of the b subunit of the *Escherichia*

528   *coli* F_1F_0-ATPase. J. Biol. Chem. 272: 21233–21239.

529 Nuckolls, N.L., M. A. B. Núñez, M. T. Eickbush, J. M. Young, J. J. Lange *et al.*, 2017. *wtf* genes

530   are prolific dual poison-antidote meiotic drivers. ELife Sciences 6: e26033.

531 Perkins, D. D., 1974 The manifestation of chromosome rearrangements in unordered asci of

532   Neurospora. Genetics 77: 459–489.

533 Raju, N. B., 1979 Cytogenetic behavior of Spore killer genes in Neurospora. Genetics 93: 607–

534   623.

535 Raju, N. B., 1980 Meiosis and ascospore genesis in Neurospora. Eur. J. Cell Biol. 23: 208–223.

536 Raju, N. B., D. D. Perkins, and D. Newmeyer, 1987 Genetically determined nonselective

537   abortion of asci in *Neurospora crassa*. Can. J. Bot. 65:1539–1549.

538   Raju, N. B., 1994   Ascomycete Spore killers: Chromosomal elements that distort genetic ratios

539   among the products of meiosis. Mycologia 86: 461–473.

540   Raju, N. B., R. L. Metzenberg, and P. K. T. Shiu, 2007   Neurospora spore killers *Sk-2* and *Sk-3*

541   suppress meiotic silencing by unpaired DNA. Genetics 176: 43–52.

542   Revington M., McLachlin D. T., Shaw G. S., Dunn S. D., 1999 The dimerization domain of the b

543   subunit of the *Escherichia coli* F(1)F(0)-ATPase. J. Biol. Chem. 274: 31094–31101.

544   Rhoades, M., 1952 Preferential Segregation in Maize, pp. 66–80 in Heterosis: a record of

545   researches directed towards explaining and utilizing the vigor of hybrids, edited by J. W.

546   Gowen. Iowa State College Press, Ames Iowa USA.

547   Samarajeewa, D. A., P. A. Sauls, K. J. Sharp, Z. J. Smith, H. Xiao *et al.*, 2014   Efficient

548   detection of unpaired DNA requires a member of the Rad54-like family of homologous

549   recombination proteins. Genetics 198: 895–904.

550   Saupe, S. J., 2011 The [Het-s] prion of *Podospora anserina* and its role in heterokaryon

551   incompatibility. Semin. Cell Dev. Biol. 22: 460–468.

552   Shiu, P. K. T., D. Zickler, N. B. Raju, G. Ruprich-Robert, and R. L. Metzenberg, 2006   SAD-2

553   is required for meiotic silencing by unpaired DNA and perinuclear localization of SAD-1

554   RNA-directed RNA polymerase. Proc. Natl. Acad. Sci. U. S. A. 103: 2243–2248.

555   Stewart A. G., Laming E. M., Sobti M., Stock D., 2014   Rotary ATPases--dynamic molecular

556   machines. Curr. Opin. Struct. Biol. 25: 40–48.

557   Sugimoto, M., 2014 Developmental genetics of the mouse *t*-complex. Genes Genet. Syst. 89:

558   109–120.

559   Thompson, J. D., D. G. Higgins, and T. J. Gibson, 1994   CLUSTAL W: improving the

560   sensitivity of progressive multiple sequence alignment through sequence weighting,

561   position-specific gap penalties and weight matrix choice. Nucleic Acids Res. 22: 4673–

562   4680.

563 Turner, B. C., 2001   Geographic distribution of Neurospora Spore killer strains and strains

564   resistant to killing. Fungal Genet. Biol. 32: 93–104.

565 Turner, B. C., and D. D. Perkins, 1979   Spore killer, a chromosomal factor in Neurospora that

566   kills meiotic products not containing it. Genetics 93: 587–606.

567 Vogel, H. J., 1956   A convenient growth medium for Neurospora (Medium N). Microb. Genet.

568   Bull. 13: 42–43.

569 Walker J. E., M. Saraste, and N. J. Gay, 1984   The unc operon. Nucleotide sequence, regulation

570   and structure of ATP-synthase. Biochim. Biophys. Acta 768: 164–200.

571 Westergaard, M., and H. K. Mitchell, 1947   Neurospora V. A synthetic medium favoring sexual

572   reproduction. Am. J. Bot. 34: 573–577.

573 Yu, J. H., Z. Hamari, K. H. Han, J. A. Seo, Y. Reyes-Domínguez *et al.*, 2004   Double-joint

574   PCR: a PCR-based molecular tool for gene manipulations in filamentous fungi. Fungal

575   Genet. Biol. 41: 973–981.

576 Zimmering, S., L. Sandler, and B. Nicoletti, 1970 Mechanisms of meiotic drive. Annu. Rev.

577   Genet. 4: 409–436.

578

579   **Figure Legends**

580   **Figure 1** Sk-2^{INS1} harbors a genetic element required for spore killing. (A) The diagram

581   illustrates phenotypic differences between spore killing and normal ascus development. Asci that

582   have undergone spore killing contain four black and four white ascospores. Viable ascospores

583   may appear tan, brown, or black, depending on their level of maturity. (B) Annotation of the

584   rfk-1 region as described by Harvey et $al.$ (2014). Genes and pseudogenes are depicted as black

585   rectangles. Gene names ($e.g.$, 6197) are listed above the rectangles. Pseudogene names are

586   appended with an asterisk. Labels $v3$, $v4$, and $v5$ mark DNA intervals of the rfk-1 region that

587   were deleted and replaced with an hph selectable marker. (C–E) The images depict asci from

588   crosses between Sk^S and Sk-2 strains lacking different intervals of Sk-2^{INS1}. The predominant

589   phenotype of the asci produced by each cross is listed above each image. Crosses are as follows:

590   (C) F2-23 × ISU-3023, (D) F2-23 × ISU-3017, and (E) F2-23 × ISU-3029.

591

592   **Figure 2** Deletion and insertion maps. (A) A diagram of Sk-2^{INS1}. (B) Ten intervals of Sk-2^{INS1}

593   were deleted and replaced with hph. For convenience, each interval is named according to its

594   deletion vector ($e.g.$, interval $v5$ is named after deletion vector v5). Orange rectangles mark

595   intervals that disrupt spore killing upon deletion. Green rectangles mark intervals that do not

596   disrupt spore killing when deleted. (C) Eight intervals of Sk-2^{INS-1}were transferred to the his-3

597   locus of an Sk^S strain. Intervals were named according to the name of the plasmid used for

598   cloning of the interval ($e.g.$, interval $AH4$ is named after plasmid pAH4). Red and blue open

599   rectangles mark killer ($i.e.$, abortion-inducing) and non-killer intervals, respectively.

600

29

601 **Figure 3** Deletion of a genetic element between pseudogene *7838*[*] and the right border of

602 *Sk-2*[INS1] eliminates spore killing. (A–I) The images depict asci from crosses between an *Sk*[S]

603 strain and an *Sk-2* mating partner lacking a specific interval of *Sk-2*[INS1]. Crosses are as follows:

604 (A) F2-26 × ISU-3311, (B) F2-26 × ISU-3313, (C) F2-23 × ISU-3315, (D) F2-26 × ISU-3318,

605 (E) F2-23 × ISU-3321, (F) F2-26 × ISU-3478, (G) F2-26 × ISU-3482, (H) F2-26 × ISU-3483,

606 and (I) F2-26 × ISU-3485.

607

608 **Figure 4** A genetic element within *Sk-2*[INS1] causes ascus abortion upon its transfer to an *Sk*[S]

609 strain. (A–H) Images depict asci from crosses between an *Sk*[S] *sad-2*[Δ] strain and an *Sk*[S] mating

610 partner carrying a specific interval of *Sk-2*[INS1]. Crosses are as follows: (A) ISU-3037 ×

611 ISU-3224, (B) ISU-3037 × ISU-3228, (C) ISU-3036 × ISU-3243, (D) ISU-3037 × ISU-3656, (E)

612 ISU-3037 × ISU-3658, (F) ISU-3036 × ISU-4269, (G) ISU-3037 × ISU-4271, and (H) ISU-3037

613 × ISU-3660.

614

615 **Figure 5** The *AH36* interval from an *rfk-1* mutant does not cause ascus abortion. Images depict

616 asci from crosses between an *Sk*[S] *sad-2*[Δ] strain and an *Sk*[S] strain carrying either the *AH36* interval

617 from (A) F2-19 (*rfk-1*[+]) or (B) ISU-3211 (an *rfk-1* mutant). Crosses are as follows: (A) ISU-3037

618 × ISU-4273 and (B) ISU-3037 × ISU-4275.

619

620 **Figure 6** The *AH36* interval from an *rfk-1* mutant contains seven point mutations. (A) The 1481

621 bp sequence of *AH36*[Sk-2] is shown. A region containing 7.17 repeats of a 46–48 bp sequence is

622 highlighted with red and blue fonts. The colors alternate with each iteration of the repeated

623 sequence. The *AH36*[3211] sequence contains seven G to A transition mutations. The position of

624   each mutation is marked by a white character on a black background with the non-mutated

625   character shown. The mutations in $AH36^{3211}$ are (from left to right): G27904A, G27945A,

626   G27972A, G28052A, G28104A, G28300A, and G28326A. A non-native promoter was placed

627   directly upstream of a putative RFK-1 start codon (white font, green background) with vector

628   v199. A non-native promoter was also placed directly upstream of a TTT triplet (white font, blue

629   background) with vector v200. (B) Alignment of the repetitive sequences highlighted in panel A.

630

631   **Figure 7** A point mutation within *AH36* eliminates its ability to abort ascus development. Six of

632   the seven point mutations in $AH36^{3211}$ were examined for a potential role in ascus abortion. Each

633   mutation was placed individually in $AH36^{Sk-2}$ by site-directed mutagenesis. (A–G) Images depict

634   asci from crosses between an Sk^S $sad-2^\Delta$ strain and an Sk^S mating partner carrying $AH36^{Sk-2}$ or

635   one of its mutated derivatives. Crosses are as follows: (A) ISU-3037 × ISU-4273, (B) ISU-3037

636   × ISU-4551, (C) ISU-3037 × ISU-4552, (D) ISU-3037 × ISU-4553, (E) ISU-3037 × ISU-4554,

637   (F) ISU-3037 × ISU-4555, (G) ISU-3037 × ISU-4556.

638

639   **Figure 8** A putative start codon for RFK-1 exists within *AH36*. (A) A DNA construct consisting

640   of *hph* and the promoter for the *N. crassa ccg-1* gene was used to make two transformation

641   vectors. (B) Vector 199 (v199) was designed to replace 133 bp of *AH36* while fusing *ccg-1*(P) to

642   a putative ATG codon at position 28,264 (Figure 6), thereby creating the $v199^A::hph-ccg-1$(P)

643   allele. Similarly, vector 200 (v200) was designed to replace 223 bp of *AH36* while fusing

644   *ccg-1*(P) to position 28,354 (Figure 6), thereby creating the $v200^A::hph-ccg-1$(P) allele. (C–E)

645   Crosses were performed to determine the effect of each allele on spore killing. Images depict asci

646   from the following crosses (C) F2-26 × P15-53, (D) F2-26 × ISU-4557, and (E) F2-26 ×

647   ISU-4558.

648

649   **Figure 9** The native arrangement of *rfk-1* protects it from MSUD. (A) Interval *AH36* spans the

650   right border of *Sk-2* (marked by a black dotted line). An *hph* selectable marker was placed

651   immediately to the right of *AH36* in an *Sk-2* strain (with vector v140) to create the *v140$^\Delta$::hph*

652   allele and at the corresponding location in an *Sk^S* strain (with vector v150) to create the

653   *v150$^\Delta$::hph* allele. (B–D) Crosses were performed to determine the effect of each allele on spore

654   killing. Images depict asci from the following crosses: (B) F2-23 × ISU-4344, (C) ISU-4348 ×

655   ISU-4344, and (D) ISU-3036 × ISU-4344.

656

657   **Figure 10** The *ncu06238* gene is not required for spore killing. (A) Asci from a cross between

658   two *Sk^S* strains (ISU-4559 × P8-43), where one of the strains has had its *ncu06238* coding

659   sequences deleted. While some normal asci are detected, many asci are abnormal and some

660   mimic the spore killer phenotype (red arrows). (B) Asci from a cross between an *Sk^S* strain and

661   an *Sk-2* strain (ISU-4559 × ISU-4561), where both strains have been deleted of their *ncu06238*

662   coding sequences. Nearly all viable progeny isolated from this cross have the *Sk-2* genotype (47

663   out of 48, data not shown).

664

665   **Figure 11** Replacement of *AH36^{3211}* with *AH36^{Sk-2}* restores spore killing to an *rfk-1* mutant. (A)

666   Strain ISU-4526 was constructed by replacing *AH36^{3211}* in ISU-3222 (upper diagram, red box)

667   with *nat1* (using vector v160; ISU-3222 is a descendant of ISU-3211). Strain ISU-4563 was then

668   constructed by replacing *AH36$^\Delta$::nat1* in ISU-4562 with *AH36^{Sk-2}::hph* (lower diagram, red box

669   and green rectangle). The locations of the two recombination flanks used to replace *AH36^Δ::nat1*

670   with *AH36^{Sk-2}::hph* are indicated with black crosses and red-dotted lines. (B–D) Asci are from

671   crosses between F2-23 and (B) ISU-3222, (C) ISU-4562, and (D) ISU-4563. (E–G) Asci are

672   from crosses between ISU-4348 and (E) ISU-3222, (F) ISU-4562, and (G) ISU-4563.

673

674   **Figure 12** RFK-1 is related to NCU07086. (A) All known *rfk-1* mutations alter the predicted

675   amino acid sequence of RFK-1. (B) A coding region of 2105 bp is predicted for gene *ncu07086*

676   (from start codon to stop codon, including introns). Predicted introns are labeled I1 through I4.

677   An AtpF Superfamily domain (NCBI CDD, Accession No. cl28522) can be identified within the

678   N-terminal end of the NCU07086 protein sequence. (C) The first 39 amino acids of RFK-1 and

679   NCU07086 are similar. (D) The repetitive sequence identified within *AH36* (see Figure 6)

680   appears to have originated from within the first intron of *ncu07086*. The first intron of ncu07086

681   is predicted to be 141 nucleotides long (NCBI Gene ID: 3876500), and only the first 84

682   nucleotides are shown. In contrast, the entire *AH36* repeat region is shown along with an

683   additional four nucleotides upstream of "repeat A". These four nucleotides include the stop

684   codon for the hypothetical 39 amino acid version of RFK-1.

685

Table 1 Strains used in this study

Name (alias)	Genotype[a]
F2-19	*rid; fl; Sk-2; A*
F2-23 (RTH1005.1)	*rid; fl A*
F2-26 (RTH1005.2)	*rid; fl a*
ISU-3017 (RKS2.1.2)	*rid$^?$; Sk-2 leu-1 v4$^\Delta$::hph; mus-51$^?$ a*
ISU-3023 (RKS1.1.6)	*rid$^?$; Sk-2 leu-1 v3$^\Delta$::hph; mus-51$^?$ a*
ISU-3029 (RKS3.2.5)	*rid; Sk-2 leu-1 v5$^\Delta$::hph; mus-51$^\Delta$:bar a*
ISU-3036 (RTH1623.1)	*rid; fl; sad-2$^\Delta$::hph A*
ISU-3037 (RTH1623.2)	*rid; fl; sad-2$^\Delta$::hph a*
ISU-3211 (RTH1158.8)	*rid; Sk-2 rsk$^\Delta$::hph rfk-1^{3211}; mus-51$^\Delta$::bar a*
ISU-3222 (RTH1249.14)	*rid; Sk-2 rfk-1^{3211}; mus-51$^\Delta$::bar a*
ISU-3223 (RTH1294.17)	*Sk-2 leu-1; mus-51$^\Delta$::bar A*
ISU-3224 (HAH8.1.3)	*rid his-3$^+$::AH4^{Sk-2}::hph; A*
ISU-3228 (HAH10.1.1)	*rid his-3$^+$::AH6^{Sk-2}::hph; A*
ISU-3243 (HAH16.1.1)	*rid his-3$^+$::AH14^{Sk-2}::hph A*
ISU-3311 (RDS1.1)	*Sk-2 leu-1 v31$^\Delta$::hph; mus-51$^\Delta$::bar A*
ISU-3313 (RDS2.3)	*Sk-2 leu-1 v32$^\Delta$::hph; mus-51$^\Delta$::bar A*
ISU-3315 (RDS3.9)	*Sk-2 leu-1 v33$^\Delta$::hph a*
ISU-3318 (RDS4.8)	*Sk-2 leu-1 v34$^\Delta$::hph A*
ISU-3321 (RDS5.9)	*rid; Sk-2 leu-1 v35$^\Delta$::hph; mus-51$^\Delta$::bar a*
ISU-3478 (RDS13.9.1)	*rid; Sk-2 v37$^\Delta$::hph; mus-51$^\Delta$::bar A*
ISU-3482 (RDS14.4.2)	*rid; Sk-2 v38$^\Delta$::hph A*
ISU-3483 (RDS15.1.1)	*rid; Sk-2 v39$^\Delta$::hph A*
ISU-3485 (RDS16.4.1)	*rid; Sk-2 v40$^\Delta$::hph A*
ISU-3656 (HAH42.1)	*rid his-3$^+$::AH30^{Sk-2}-hph A*
ISU-3658 (HAH43.1)	*rid his-3$^+$::AH31^{Sk-2}-hph A*
ISU-3660 (HAH44.1)	*rid his-3$^+$::AH32^{Sk-2}-hph A*
ISU-4269 (RAH64.1.1)	*rid his-3$^+$::AH37^{Sk-2}-hph; mus-52$^\Delta$::bar a*

1

ISU-4271 (RAH63.1.2)	*rid his-3$^+$::AH36^{Sk-2}-hph; mus-52$^\Delta$::bar A*
ISU-4273 (HNR12.6.1)	*rid his-3$^+$::AH36^{Sk-2}-hph A*
ISU-4275 (HNR10.4.2)	*rid his-3$^+$::AH36^{3211}-hph A*
ISU-4344 (RAY1.13)	*rid; Sk-2 v140$^\Delta$::hph; mus-51$^\Delta$::bar A*
ISU-4348 (RAY6.5)	*rid; fl; v150$^\Delta$::hph a*
ISU-4551 (RNR29.1)	*rid his-3$^+$::AH36$^{Sk-2[G27945A]}$-hph; mus-52$^?$ A*
ISU-4552 (RNR28.1)	*rid his-3$^+$::AH36$^{Sk-2[G27972A]}$-hph; mus-52$^?$ A*
ISU-4553 (RNR27.1)	*rid his-3$^+$::AH36$^{Sk-2[G28052A]}$-hph; mus-52$^?$ A*
ISU-4554 (RNR26.1)	*rid his-3$^+$::AH36$^{Sk-2[G28104A]}$-hph; mus-52$^?$ A*
ISU-4555 (RNR25.1)	*rid his-3$^+$::AH36$^{Sk-2[G28300A]}$-hph; mus-52$^?$ A*
ISU-4556 (RNR30.1)	*rid his-3$^+$::AH36$^{Sk-2[G28326A]}$-hph; mus-52$^?$ A*
ISU-4557 (RNR129.1.3)	*rid; Sk-2 v199$^\Delta$::hph-ccg-1(P); mus51$^?$ A*
ISU-4558 (RNR130.1.3)	*rid; Sk-2 v200$^\Delta$::hph-ccg-1(P); mus51$^?$A*
ISU-4559 (RNR108.1.12)	*rid; fl; ncu06238$^\Delta$::hph mus-52$^\Delta$::bar a*
ISU-4561 (RNR109.3.2)	*rid; Sk-2 ncu06238$^\Delta$::hph; mus51$^\Delta$::bar A*
ISU-4562 (HNR92.1)	*rid; Sk-2 v160$^\Delta$::nat1; mus-51$^\Delta$::bar a*
ISU-4563 (HNR100.11.1)	*rid; Sk-2 v140$^\Delta$::hph; mus-51$^\Delta$::bar a*
P8-42	*rid; mus-51$^\Delta$::bar a*
P8-43	*rid; mus-52$^\Delta$::bar A*
P15-53 (RTH1122.22)	*rid; Sk-2; mus-51$^\Delta$::bar A*

[a]The *rid$^?$*, *mus-51$^?$* and *mus-52$^?$* designations are used if the genotype has not been determined for the indicated allele. Genotypes of all key alleles were determined by PCR or lineage analysis.

Table 2 Interval positions

name	start	stop
Miscellaneous intervals of the 45 kb rfk-1 region		
$Sk\text{-}2^{INS1}$	18118	29151
rfk-1 coding[a]	28264	28383
repeats[b]	28384	28722
Intervals deleted from the 45 kb rfk-1 region		
v3	15640	15664
v4	36166	36426
v5	18042	28759
v31	18042	21464
v32	18042	25268
v33	18042	26951
v34	18042	27667
v35	25837	28759
v37	27242	28759
v38	27602	28759
v39	28126	28759
v40	27602	28198
v140	29381	29401
v160	27740	29401
v175	29489	31883
v199	28131	28263
v200	28131	28353
Intervals transferred from the 45 kb rfk-1 region to Sk^{S}		
AH4	16579	22209
AH6	19408	25648
AH14	25632	28324
AH30	27528	29702
AH31	27900	29702
AH32	28304	29702
AH36	27900	29380
AH37	27900	29512

The coordinates of each interval are as defined by GenBank sequence KJ908288.1. [a]hypothetical. [b]contains repeats of a 47 bp sequence.

Figure 1

A

B

C 4B:4W

$Sk^S × Sk-2 v3^Δ$

D 4B:4W

$Sk^S × Sk-2 v4^Δ$

E 8B:0W

$Sk^S × Sk-2 v5^Δ$

Figure 2

Figure 2

Figure 3

A 4B:4W

$Sk^S \times Sk$-2 $v31^\Delta$

B 4B:4W

$Sk^S \times Sk$-2 $v32^\Delta$

C 4B:4W

$Sk^S \times Sk$-2 $v33^\Delta$

D 4B:4W

$Sk^S \times Sk$-2 $v34^\Delta$

E 8B:0W

$Sk^S \times Sk$-2 $v35^\Delta$

F 8B:0W

$Sk^S \times Sk$-2 $v37^\Delta$

G 8B:0W

$Sk^S \times Sk$-2 $v38^\Delta$

H 8B:0W

$Sk^S \times Sk$-2 $v39^\Delta$

I 8B:0W

$Sk^S \times Sk$-2 $v40^\Delta$

Figure 4

A 8B:0W

Sk^S sad-2$^\Delta$ × Sk^S AH4^{Sk-2}

B 8B:0W

Sk^S sad-2$^\Delta$ × Sk^S AH6^{Sk-2}

C 8B:0W

Sk^S sad-2$^\Delta$ × Sk^S AH14^{Sk-2}

D aborted

Sk^S sad-2$^\Delta$ × Sk^S AH30^{Sk-2}

E aborted

Sk^S sad-2$^\Delta$ × Sk^S AH31^{Sk-2}

F aborted

Sk^S sad-2$^\Delta$ × Sk^S AH37^{Sk-2}

G aborted

Sk^S sad-2$^\Delta$ × Sk^S AH36^{Sk-2}

H 8B:0W

Sk^S sad-2$^\Delta$ × Sk^S AH32^{Sk-2}

Figure 5

A aborted

B 8B:0W

Sk^S $sad\text{-}2^\Delta$ ×
Sk^S $AH36^{Sk\text{-}2}$

Sk^S $sad\text{-}2^\Delta$ ×
Sk^S $AH36^{3211}$

Figure 6

A

CATTGATACCGAGTCTTTCCGTTCTTAAGGTTGGAGTGAGGATATGATCCGGCACGTCGAAGGAGGAACTAT
GGTAAATAAGTCAGTCATCATCAAGGAAAAGAACAGTATTAGGTGCCTTCAAGTTACCTACCTTCTCCGACG
GGGGCCCTGCCTTCCCTTAGTTCTCTCATGAAGCTGGAAGTTATATCCTAACCCACTACTGACAAAACAAAG
CAAGAGCTGCTGCCCCAACTATAGACAGCACGCTTTTCCACCTCAGTTGGGGCACCTAGAAAGCTATAAGAT
CCCTCTTCCCCCGGCCCAACCTCTCCTCAGAATTTCTTTTTTTCTCCAACATTGTTAAGAACTTTGTTTTTG
GAAAATGGCCTGCCCCACAGGGTTTTTTTACCGCTCTTTTTGGCAAACTCCTCACCATCCCCATTTGGGTGTT
GGTGTTTGTATTCAATGCTCTGTTTGTCTTCCCCCGGTTTTGGGTCTGGTAAGTCTCCTTCATGTTCCAATT
CATTTTTGTTTTTTCCTTTCTCTTCTCGTCTCCTTCATGTTCCAATTCATTTTTGTTTTTTTCCTTTCTCTT
CTCGTCTCCTTCATGTTCCAGTTCATTTTTGTTTTTTCCTTTCTCTTCTCGTCTCCTTCATGTTCCAATTCA
TTTTTGTTTTTTTCCTTTCTCTTCTCGTCTCCTTCATGTTCCAGTTCATTTTTGTTTTTTCCTTTCTCTTCT
CGTCTCCTTCATGTTCCAATTCATTTTTGTTTTTTTCCTTTCTCTTCTCGTCTCCTTCATGTTCCAATTCAT
TTTTTTTGTCCTTTCTCTTCTCGTCTCCTTACAGTTTACCTTATCCTCTCGGTCCTCTCTGTCTTTCGCTA
ACCAGGAACAGGCGCTTACCACCACGGCTGCAACACGAGCAGCAGCAGCAGGACCGGAACGATGACGAATGG
CAGCGGCAGCAACAGGACAGGCGGGTTGTGGTTTGGCACCCACCGCCCCCTCCAGACGTGGAGATGGCCCTC
CAAGACAATCCCACTGCCGCCCCCGCAGAGCCGGCTGACCTCGACCACCCAGCGCCGTAGTGGCGGCGCTGG
GTGGCCGACGAGTAGGTCAATGCTATTCCCAGATTATGAAATGTATCGCTGACAGTTGCACACCAGTGCCTA
CCCGGCCGTCCACTTCTGCGTGACCGCAGCCAATGCGGTCACGCAGGGGTTGTAATTCCACGTGAGCATTCC
CCACCTTCTCTCGGGACCGACTTCCGTATCAACCCCAAATTTATCGGACTGACCCGTCCGAATCAAGGCGAA
CCGAGAGGACACAGACAAGGCCCACGTCCGCCATCAGCATTCCCAGCTGGCCGACCGCACCGCCGCAACTCC
CACTTTACCTCAACACCAGAATACGGAATCGGTACATCGACAGCAGCATCATCATCATCAATATCACCACCT
CCACTTGGCGCGCACTTGCGGAAAACGTCCCGCTACACCGT

B

```
Repeat A  GTCTCCTTCATGTTCCAATTCATTTTTG-TTTTTTCCTTTCTCTTCTC  28430
Repeat B  GTCTCCTTCATGTTCCAATTCATTTTTGTTTTTTTCCTTTCTCTTCTC  28478
Repeat C  GTCTCCTTCATGTTCCAGTTCATTTTTG-TTTTTTCCTTTCTCTTCTC  28525
Repeat D  GTCTCCTTCATGTTCCAATTCATTTTTGTTTTTTTCCTTTCTCTTCTC  28573
Repeat E  GTCTCCTTCATGTTCCAGTTCATTTTTG-TTTTTTCCTTTCTCTTCTC  28260
Repeat F  GTCTCCTTCATGTTCCAATTCATTTTTGTTTTTTTCCTTTCTCTTCTC  28668
Repeat G  GTCTCCTTCATGTTCCAATTCATTTTT--TTTTGTCCTTTCTCTTCTC  28714
Repeat H  GTCTCCTT----------------------------------------  28722
```

Figure 7

A aborted

Sk^S sad-2^Δ ×
Sk^S $AH36^{Sk\text{-}2}$

B aborted

Sk^S sad-2^Δ ×
Sk^S $AH36^{Sk\text{-}2[G27945A]}$

C aborted

Sk^S sad-2^Δ ×
Sk^S $AH36^{Sk\text{-}2[G27972A]}$

D aborted

Sk^S sad-2^Δ ×
Sk^S $AH36^{Sk\text{-}2[G28052A]}$

E aborted

Sk^S sad-2^Δ ×
Sk^S $AH36^{Sk\text{-}2[G28104A]}$

F aborted

Sk^S sad-2^Δ ×
Sk^S $AH36^{Sk\text{-}2[G28300A]}$

G 8B:0W

Sk^S sad-2^Δ ×
Sk^S $AH36^{Sk\text{-}2[G28326A]}$

Figure 8

A *hph-ccg-1*(P) DNA construct

hph   *ccg-1*(P)

B *Sk-2 AH36 locus*

7838*Sk-2   *AH36Sk-2*   *6238Sk-2*

↑ATG(28,264)

v199
v200

0.5 kb

C 4B:4W   D 4B:4W   E 8B:0W

SkS × Sk-2

SkS × Sk-2
v199Δ::hph-ccg-1(P)

SkS × Sk-2
v200Δ::hph-ccg-1(P)

Figure 9

A

no homology   94.4% identical DNA sequence

Sk-2: *4949*   7838* AH36*   *6238*   *6239*

↑v140
hph

Sk^S: *6237*   *6238*   *6239*

↑v150
hph

1 kb

B 8B:0W   **C** 4B:4W   **D** 4B:4W

Sk^S ×
Sk-2 v140^Δ::hph

Sk^S v150^Δ::hph ×
Sk-2 v140^Δ::hph

Sk^S sad-2^Δ×
Sk-2 v140^Δ::hph

Figure 10

A

B

Sk^S 6238^Δ × Sk^S Sk^S 6238^Δ × Sk-2 6238^Δ

Figure 11

A

B 8B:0W

Sk^S ×
Sk-2 AH36^{3211}

C 8B:0W

Sk^S ×
Sk-2 AH36^Δ::nat1

D 8B:0W

Sk^S ×
Sk-2 AH36^{Sk-2}::hph

E 8B:0W

Sk^S v150^Δ::hph ×
Sk-2 AH36^{3211}

F 8B:0W

Sk^S v150^Δ::hph ×
Sk-2 AH36^Δ::nat1

G 4B:4W

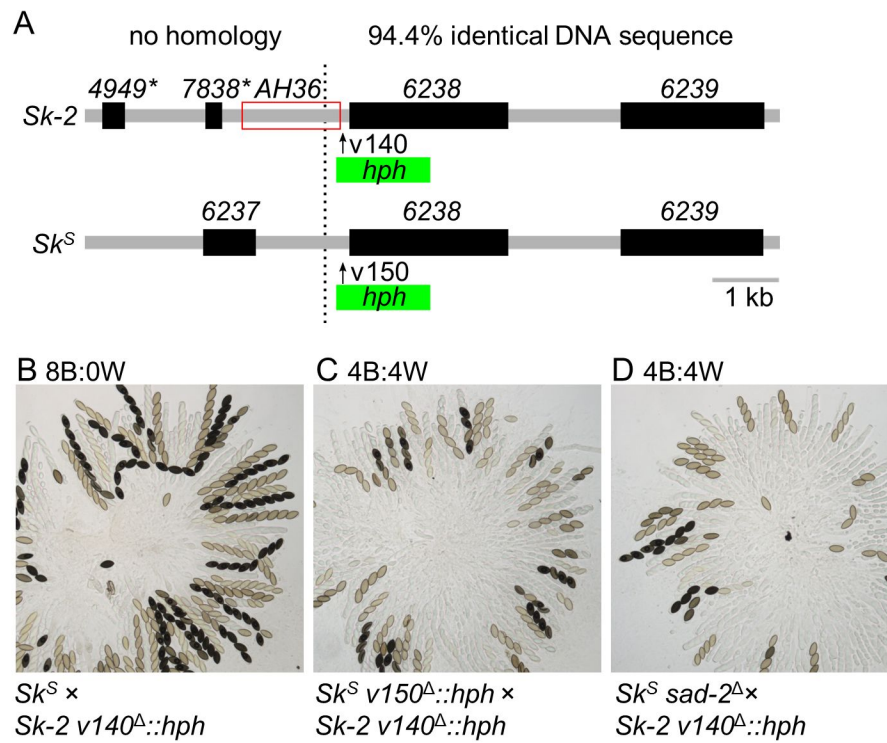*Sk^S v150^Δ::hph* ×
Sk-2 AH36^{Sk-2}::hph

Figure 12

A

```
RFK-1       MACPTGFFTALFGKLLTIPIWVLVFVFNALFVFPRFWVW*  40
RFK-1 3211  MACPTGFFTALFSKLLTIPI*VLVFVFNALFVFPRFWVW*  40
RFK-1 3212  MACPTGFFYRSFWQTPHHPHLGVGVCIQCSVCLPPVLGLV  40
RFK-1 3213  MACPTGFFTALFGKLLTIPIWVLVFVFNTLFVFPRFWVW*  40
```
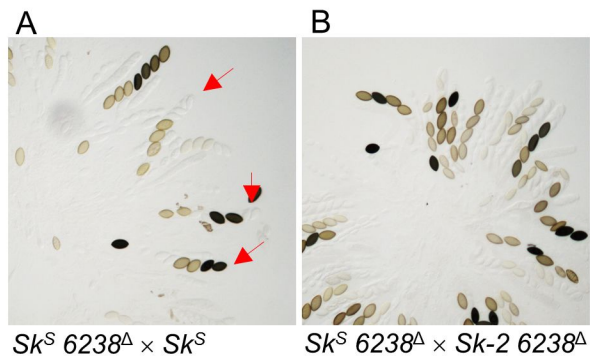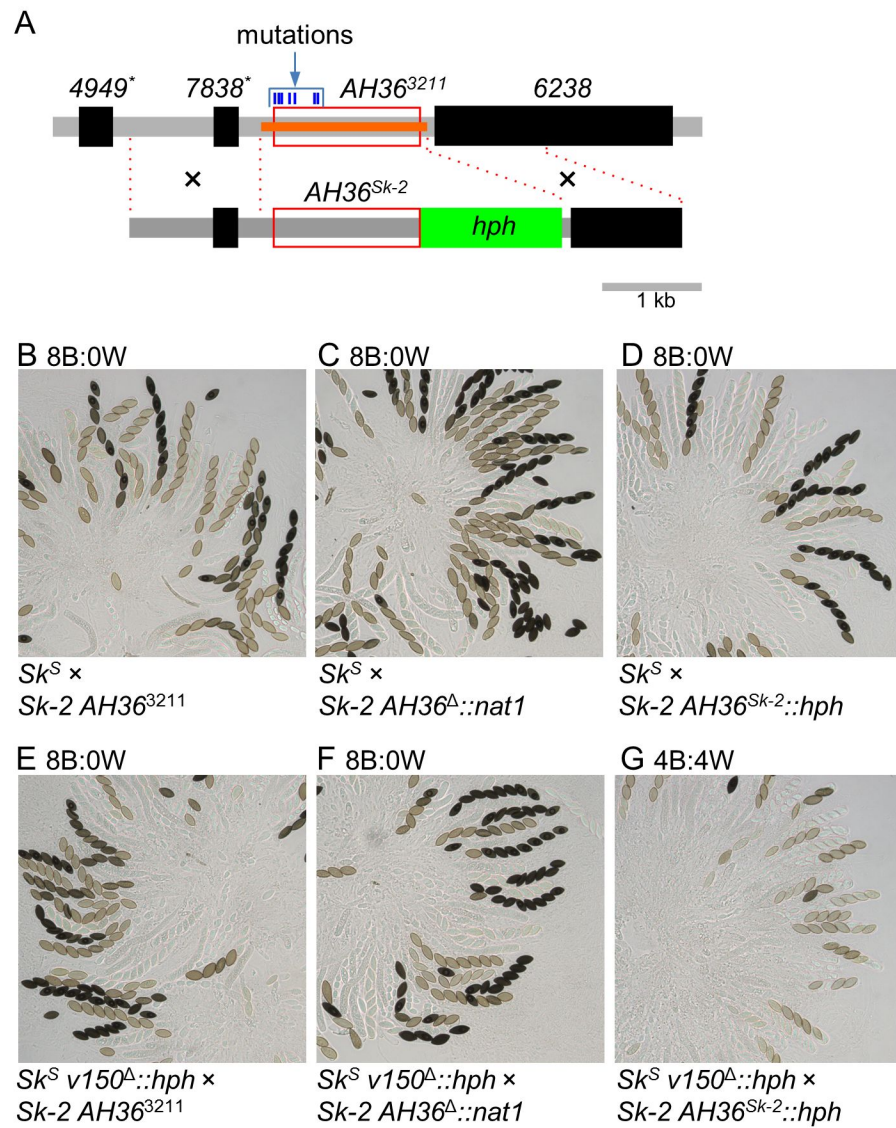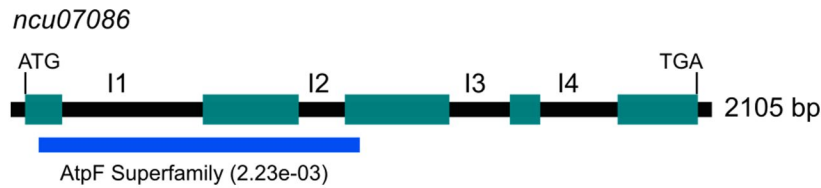
B

ncu07086

AtpF Superfamily (2.23e-03)

C

```
RFK-1      MACPTGFFTALFGKLLTIPIWVLVFVFNALFVFPRFWVW*  40
NCU07086   MTCLNAFLTALFGKVLSAFIWLGVFAWNVYFVWPGWPLLN  40
```

D

stop codon for 39 aa RFK-1 model

```
                  Repeat A                                                    Repeat B
rfk-1  GTAAGTCTCCTTCATGTTCCAATTCATTTTTGTTTTTTCCTTTCTCTTCTCGTCTCCTTCATGTTCCAAT  28449
7086   GTAAGTCTACTCTATATTCCAATTCATTTTTGGTTTTTCCGTTCTCTTCTC--------------------  51

                                              Repeat C
rfk-1  TCATTTTTGTTTTTTTCCTTTCTCTTCTCGTCTCCTTCATGTTCCAGTTCATTTTTGTTTTTTCCTTTCT  28519
7086   ---------------------------------------------------------------------  51

              Repeat D                                            Repeat E
rfk-1  CTTCTCGTCTCCTTCATGTTCCAATTCATTTTTGTTTTTTTCCTTTCTCTTCTCGTCTCCTTCATGTTCC  28589
7086   ---------------------------------------------------------------------  51

                                  Repeat F
rfk-1  AGTTCATTTTTGTTTTTTTCCTTTCTCTTCTCGTCTCCTTCATGTTCCAATTCATTTTTGTTTTTTTCCTT  28659
7086   ----------------------------------------------------------------------  51

          Repeat G                                              Repeat H
rfk-1  TCTCTTCTCGTCTCCTTCATGTTCCAATTCATTTTTTTTTGTCCTTTCTCTTCTCGTCTCCTTACAGTTT  28729
7086   ------------------------------------------------------GTCTCCTTACAGTTT  66

rfk-1  ACCTTATCCTCTCGGTCC  28747
7086   ACCTTGCCCTTTCGATCC  84
```

Supporting Information

Rhoades *et al*. "Identification of a genetic element required for spore killing in Neurospora".

Contents

Figure S1. Unpaired Sk-2^{INS1}-intervals do not kill ascospores in MSUD-proficient crosses.

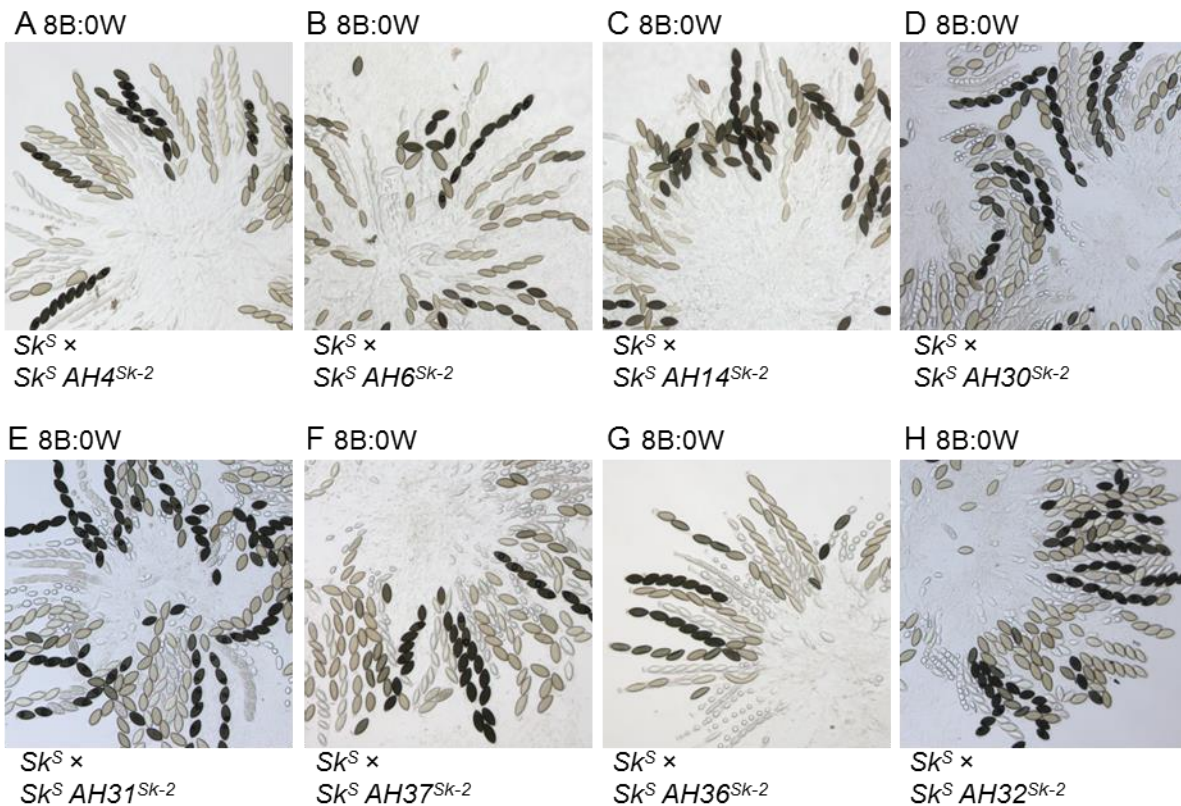Table S1. Primers for DJ-PCR-based construction of deletion vectors.

Table S2. Primers for DJ-PCR center products.

Table S3. Primers for cloning Sk-2 intervals to pTH1256.1.

Table S4. Primers for amplification of $AH36^{Sk-2}$::hph.

Table S5. Primers for site directed mutagenesis of $AH36^{Sk-2}$.

Figure S1 Unpaired $Sk\text{-}2^{INS1}$-intervals do not kill ascospores in MSUD-proficient crosses.

Unpaired $Sk\text{-}2^{INS1}$-intervals do not kill ascospores in MSUD-proficient crosses. (A–H) The images depict asci from crosses between Sk^S strains, one of which carries an interval of the $Sk\text{-}2^{INS1}$ locus (*e.g.*, $AH4^{Sk\text{-}2}$, $AH6^{Sk\text{-}2}$, etc.). All crosses produced asci with an 8B:0W phenotype. Crosses are as follows: (A) F2-26 × ISU-3224, (B) F2-26 × ISU-3228, (C) F2-23 × ISU-3243, (D) F2-26 × ISU-3656, (E) F2-26 × ISU-3658, (F) F2-23 × ISU-4269, (G) F2-26 × ISU-4271, and (H) F2-26 × ISU-3660.

Table S1 Primers for DJ-PCR-based construction of deletion vectors.

Nineteen deletion vectors were constructed by double joint (DJ)-PCR (Yu *et al.* 2004; Hammond *et al.* 2011). The table below lists the forward and reverse primer sequences (5′ to 3′) for the left recombination flank (L), the right recombination flank (R), and the nested amplification of each completed vector (N).

For each vector, the left and right DNA flanks were amplified from genomic DNA of the transformation host, which is also indicated in the table.

The center fragment for each vector is listed next to the name of each vector in the left-most column. Center fragments were either *hph*, *nat1*, or *hph-ccg-1*(P). See Table S2 for more information on the center fragments.

Vector (*center*) Primer numbers	*Name of transformation host* Primer sequences	Primer purpose
v3 (*hph*)	*Transformation host: ISU-3223*	
73	CAAGACCCAGAACAACGCCAACA	L
74	AAAAAATGCTCCTTCAATATCAGTTCCTCGCTCCTCTTCCGCAAATTA	L
75	GAGTAGATGCCGACCGGGAACCAGTTTGGTGGGATACTCGGTGCAGGTA	R
76	CGACACCTCGAATACGCCCTCTC	R
77	CCGGAAACGTCAGCAAACACGTA	N
78	GCGCCAGCTCCTCTACACTCTCC	N
v4 (*hph*)	*Transformation host: ISU-3223*	
79	CCAAGCCAAACTCAAGGGAATCG	L
80	AAAAAATGCTCCTTCAATATCAGTTAATGGCGGTGATCTTCGACTGCT	L
81	GAGTAGATGCCGACCGGGAACCAGTTGCCCAGACTCAGCTTGCATTGAC	R
82	TCACCTTGGCCCTGGAGTACCTG	R
83	CAAACGGGACGCAACCTCTATGA	N
84	CCAAGCGGGTTCCAGATAAGACG	N
v5 (*hph*)	*Transformation host: ISU-3223*	
85	CACCATGTAGTCGGAGCGGAAGA	L
86	AAAAAATGCTCCTTCAATATCAGTTTCATCTTGACGGGCAGAACTGAA	L
87	GAGTAGATGCCGACCGGGAACCAGTTGCTAACCAGGAACAGGCGCTTACC	R
88	CATCGAAAGGGAGAGGCACTTCG	R
89	GCCTTCCTTCTTCACACGGAGGT	N
90	ACAGGATCTGGTCATCCCGCTTC	N
v31 (*hph*)	*Transformation host: ISU-3223*	
85	CACCATGTAGTCGGAGCGGAAGA	L
86	AAAAAATGCTCCTTCAATATCAGTTTCATCTTGACGGGCAGAACTGAA	L
167	GAGTAGATGCCGACCGGGAACCAGTTATTGAGGTGAGGACAAGCGATGA	R
168	CATACGGCCCATGTTACCGCACT	R
89	GCCTTCCTTCTTCACACGGAGGT	N
170	CAACGAAGCAGGCTCCCATACAG	N
v32 (*hph*)	*Transformation host: ISU-3223*	
85	CACCATGTAGTCGGAGCGGAAGA	L
86	AAAAAATGCTCCTTCAATATCAGTTTCATCTTGACGGGCAGAACTGAA	L
173	GAGTAGATGCCGACCGGGAACCAGTTGTCGTCCGTGAATCGTGATCCTT	R
174	AATTCGCCGTGTACTTCGCTGTG	R
89	GCCTTCCTTCTTCACACGGAGGT	N
176	CGGTTGTATCTGCCGGTTTGAAGA	N
v33 (*hph*)	*Transformation host: ISU-3223*	
85	CACCATGTAGTCGGAGCGGAAGA	L
86	AAAAAATGCTCCTTCAATATCAGTTTCATCTTGACGGGCAGAACTGAA	L
3	GAGTAGATGCCGACCGGGAACCAGTTCATGGCAGTGAAGTGGACAAGCTG	R
4	GTGGTAAGCGCCTGTTCCTGGTTAG	R
89	GCCTTCCTTCTTCACACGGAGGT	N
6	TGCGGCCTGTTTACGAAATCCAA	N
v34 (*hph*)	*Transformation host: ISU-3223*	
85	CACCATGTAGTCGGAGCGGAAGA	L

86	AAAAAATGCTCCTTCAATATCAGTTTCATCTTGACGGGCAGAACTGAA	L
9	GAGTAGATGCCGACCGGGAACCAGTTCTCGATTGCCCGACACCTTCTGT	R
4	GTGGTAAGCGCCTGTTCCTGGTTAG	R
89	GCCTTCCTTCTTCACACGGAGGT	N
11	CGAAAGACAGAGAGGACCGAGAGGA	N
v35 (*hph*)	*Transformation host: ISU-3223*	
1	TCGGAAGGATTGCTGACTTGTGTGT	L
2	CCAAAAAATGCTCCTTCAATATCAGTTAGTTGGTAGCTGGCGCGGAAAG	L
87	GAGTAGATGCCGACCGGGAACCAGTTGCTAACCAGGAACAGGCGCTTACC	R
88	CATCGAAAGGGAGAGGCACTTCG	R
5	GCGCAGACGAACATCAAGGAGAA	N
90	ACAGGATCTGGTCATCCCGCTTC	N
v37 (*hph*)	*Transformation host: P15-53*	
7	GGCAGATACAACCGACGACCAAA	L
8	CCAAAAAAATGCTCCTTCAATATCAGTTTCCGTTTCGCTTATGATGTTAATGATG	L
87	GAGTAGATGCCGACCGGGAACCAGTTGCTAACCAGGAACAGGCGCTTACC	R
88	CATCGAAAGGGAGAGGCACTTCG	R
10	CACGTAGGGAAGGAGGTTGAAGGT	N
90	ACAGGATCTGGTCATCCCGCTTC	N
v38 (*hph*)	*Transformation host: P15-53*	
309	ACGCCAAAAGGTGTAGGGGGATT	L
310	CCAAAAAAATGCTCCTTCAATATCAGTTGACCGAACAACCGGAATGACCT	L
87	GAGTAGATGCCGACCGGGAACCAGTTGCTAACCAGGAACAGGCGCTTACC	R
88	CATCGAAAGGGAGAGGCACTTCG	R
311	AGGTCCGCAACTATTGTCCGTTT	N
90	ACAGGATCTGGTCATCCCGCTTC	N
v39 (*hph*)	*Transformation host: P15-53*	
309	ACGCCAAAAGGTGTAGGGGGATT	L
312	CCAAAAAAATGCTCCTTCAATATCAGTTGCAGCTCTTGCTTTGTTTTGTCAGT	L
87	GAGTAGATGCCGACCGGGAACCAGTTGCTAACCAGGAACAGGCGCTTACC	R
88	CATCGAAAGGGAGAGGCACTTCG	R
311	AGGTCCGCAACTATTGTCCGTTT	N
90	ACAGGATCTGGTCATCCCGCTTC	N
v40 (*hph*)	*Transformation host: P15-53*	
309	ACGCCAAAAGGTGTAGGGGGATT	L
310	CCAAAAAAATGCTCCTTCAATATCAGTTGACCGAACAACCGGAATGACCT	L
313	GAGTAGATGCCGACCGGGAACCAGTTCGGCCCAACCTCTCCTCAGAAT	R
88	CATCGAAAGGGAGAGGCACTTCG	R
311	AGGTCCGCAACTATTGTCCGTTT	N
90	ACAGGATCTGGTCATCCCGCTTC	N
v140 (*hph*)	*Transformation host: P15-53*	
1303	AACCAGGAACAGGCGCTTACCAC	L
1304	AAAAAAATGCTCCTTCAATATCAGTTACGGTGTAGCGGGACGTTTTC	L
1305	GAGTAGATGCCGACCGGGAACCAGTTTCAACAAAGCGCGTGATCTTTCG	R
871	GAACTCGAACCACTCCACGCAAA	R
1306	ACAGGACAGGCGGGTTGTGGTTT	N
872	CATGTCGGTCTTGAGGTCGTTGC	N
v150 (*hph*)	*Transformation host: P8-43*	
1332	CCGCGAATGGTTAACTGCACGGC	L
1304	AAAAAAATGCTCCTTCAATATCAGTTACGGTGTAGCGGGACGTTTTC	L
1305	GAGTAGATGCCGACCGGGAACCAGTTTCAACAAAGCGCGTGATCTTTCG	R
1333	GTCGGCATAGGCTGTGGTGGTCG	R
1334	ATGCGGCCTTGATGCACTGGCTG	N
1335	CGAGAGGGAGAGGCACTTCGCCA	N
v160 (*nat1*)	*Transformation host: ISU-3222*	
10	CACGTAGGGAAGGAGGTTGAAGGT	L
869	TGAATGCTAAAAGACACCATTTCCCACACTCCCTCAGCAAGTAAGCCGGTCACGATCC	L
870	GCTGGCTGCAATACAAGCGTTCCCACCTAACCAACTCAACAAAGCGCGTGATCTTTCG	R
871	GAACTCGAACCACTCCACGCAAA	R
311	AGGTCCGCAACTATTGTCCGTTT	N
872	CATGTCGGTCTTGAGGTCGTTGC	N

v175 (*hph*)	*Transformation host: ISU-3222*	
1433	GGAACAGGCGCTTACCACCA	L
1434	AAAAAATGCTCCTTCAATATCAGTTTGAAATGTTGATGCCTCCCTGGAT	L
1435	GAGTAGATGCCGACCGGGAACCAGTTGGGGTTTAGGGAGGGCTGCAT	R
1436	TTCCTTTCCCGCTCCGTTCG	R
1437	ACAGGACAGGCGGGTTGTGG	N
1438	CCGAATACCGACCCCCGATT	N
v176 (*hph*)	*Transformation host: P8-43*	
1439	TGGCAGGTCAAGGTCGATTGC	L
1440	AAAAAATGCTCCTTCAATATCAGTTTGAAATGTTGATGCCTCCCTAGAT	L
1441	GAGTAGATGCCGACCGGGAACCAGTTGGGGTTTAGGCAGGGCTGGAT	R
1442	TTCCTTTCCCGCTCCTTTCG	R
1443	CGGCCGCGAATGGTTAACTG	N
1438	CCGAATACCGACCCCCGATT	N
v199 [*hph-ccg-1*(P)]	*Transformation host: P15-53*	
1538	CGAAGGACAAGAGGAACGGGAAA	L
1539	GCAGCCTGAATGGCGAATGGACGCGCGGGCAGCAGCTCTTGCTTTGTTT	L
1544	TTCACAACCCCTCACATCAACCAAAATGGCCTGCCCCACAGGGTTT	R
1541	GTCACGGTGTAGCGGGACGTTTT	R
1542	GGGGCGGAGAGGAGAAGATGAGT	N
1543	GGAATTACAACCCCTGCGTGACC	N
v200 [*hph-ccg-1*(P)]	*Transformation host: P15-53*	
1538	CGAAGGACAAGAGGAACGGGAAA	L
1539	GCAGCCTGAATGGCGAATGGACGCGCGGGCAGCAGCTCTTGCTTTGTTT	L
1540	TTCACAACCCCTCACATCAACCAAATTTGTCTTCCCCCGGTTTTGG	R
1541	GTCACGGTGTAGCGGGACGTTTT	R
1542	GGGGCGGAGAGGAGAAGATGAGT	N
1543	GGAATTACAACCCCTGCGTGACC	N

Table S2 Primers for DJ-PCR center products.

The forward and reverse primers used to amplify the center fragments for construction of DJ-PCR deletion vectors are described below.

Center Primer number	*Name of template* Primer sequences
hph	*pTH1256.1(GenBank MH550659)*
12	AACTGATATTGAAGGAGCATTTTTTGG
13	AACTGGTTCCCGGTCGGCAT
nat1	*pNR28.12 (GenBank MH553564)*
297	GAGGGAGTGTGGGAAATGGTGTC
298	GTTGGTTAGGTGGGAACGCTTGT
hph-ccg-1(P)	*pTH1117.12 (GenBank JF749202)*
550	GCGCGTCCATTCGCCATTCA
1555	TTTGGTTGATGTGAGGGGTTGTGA

Table S3 Primers for cloning *Sk-2* intervals to pTH1256.1.

Eight intervals of *Sk-2*[INS1] were cloned to the *Not*I site of pTH1256.1 (GenBank MH550659), using the primers listed below. These cloning procedures created plasmids pAH4, pAH6, pAH14, pAH30, pAH31, pAH32, pAH36, and pAH37. Each plasmid was then used to transform strain P8-43.

Plasmid name Primer number	*Name of transformation host* Primer sequences
pAH4 248 249	*Transformation host: P8-43* AAAAGCGGCCGCAGGGTGGTGTGGGTGAGGATGT TTTTGCGGCCGCGAGCGGAAGTGTTTGCTTGTGTGA
pAH6 252 253	*Transformation host: P8-43* AAAAGCGGCCGCATCGCCAACGGGCATTCAAG AAAAGCGGCCGCACCCGCCTACACATGCACCATC
pAH14 302 314	*Transformation host: P8-43* AAAAGCGGCCGCTGCATGTGTAGGCGGGTATTGTG AAAAGCGGCCGCGGGGCAGGGCAGCAAGTAAG
pAH30 304 251	*Transformation host: P8-43* AAAAGCGGCCGCGAGGACCAGCTCGACGGTAGTAGG AAAAGCGGCCGCGAGGAATAGGACGTGAGGGTGTGG
pAH31 353 251	*Transformation host: P8-43* TTTTGCGGCCGCCATTGATACCGAGTCTTTCCGTTC AAAAGCGGCCGCGAGGAATAGGACGTGAGGGTGTGG
pAH32 351 251	*Transformation host: P8-43* AAAAGCGGCCGCAACTCCTCACCCATCCCCATTTG AAAAGCGGCCGCGAGGAATAGGACGTGAGGGTGTGG
pAH36 353 639	*Transformation host: P8-43* TTTTGCGGCCGCCATTGATACCGAGTCTTTCCGTTC AAAAGCGGCCGCGACGGTGTAGCGGGACGTTTTCC
pAH37 353 640	*Transformation host: P8-43* TTTTGCGGCCGCCATTGATACCGAGTCTTTCCGTTC AAAAGCGGCCGCGTTCGCTGACTTTCCCGACCA

Table S4 Primers for amplification of *AH36^{Sk-2}::hph*.

The *AH36^{Sk-2}::hph* allele was amplified from ISU-4344 using the primers 10 and 871. These primers span the *v140$^\Delta$::hph* allele in ISU-4344 and produce a PCR product containing *AH36^{Sk-2}* and *hph* between recombination flanks suitable for replacing *AH36$^\Delta$::nat1* in ISU-4562 with *AH36^{Sk-2}::hph*.

Target Primer number	Template; *Name of transformation host* Sequence
AH36^{Sk-2}::hph	Amplify from ISU-4344; *Transformation host: ISU-4562*
10	CACGTAGGGAAGGAGGTTGAAGGT
871	GAACTCGAACCACTCCACGCAAA

Table S5. Primers for site directed mutagenesis of *AH36^{Sk-2}*.

Site directed mutagenesis was performed essentially as described for the QuikChange II Site-Directed Mutagenesis Kit (Revision E.01, Agilent Technologies). The *AH36* interval from *Sk-2* was cloned to the *Not*I site of a standard 3 kb bacterial cloning vector with primers 353 and 639 (Table S2). Site-specific mutations were introduced into the resulting plasmid (pNR9.1) by PCR with the primer sets described below. PCR products were digested with *Dpn*I and used to transform chemically-competent *E. coli* Ig™ 5-alpha cells (Intact Genomics). Site directed mutations were confirmed by Sanger sequencing and mutated plasmids were used to transform P8-43.

Purpose of primers Primer number	Primer sequences
Change G to A at position 27945	
1138	GTTGGAGTGAGGATATAATCCGGCACGTCGAAG
1139	CTTCGACGTGCCGGATTATATCCTCACTCCAAC
Change G to A at position 27972	
1136	GATGATGACTGACTTATTTACTATAGTTCCTCCTTCGACGT
1137	ACGTCGAAGGAGGAACTATAGTAAATAAGTCAGTCATCATC
Change G to A at position 28052	
1134	CGACGGGGGCCCTACCTTCCCTTAGTT
1135	AACTAAGGGAAGGTAGGGCCCCCGTCG
Change G to A at position 28104	
1132	CTAACCCACTACTAACAAAACAAAGCAAGAGCTGCTGC
1133	GCAGCAGCTCTTGCTTTGTTTTGTTAGTAGTGGGTTAG
Change G to A at position 28300	
1130	GGGATGGTGAGGAGTTTGCTAAAAAGAGCGGTAAAAAAC
1131	GTTTTTTACCGCTCTTTTTAGCAAACTCCTCACCATCCC
Change G to A at position 28326	
1128	GAATACAAACACCAACACTCAAATGGGGATGGTGAG
1129	CTCACCATCCCCATTTGAGTGTTGGTGTTTGTATTC